# Meteorological and glaciological investigations on a blue ice area in the Heimefrontfjella, Dronning Maud Land, Antarctica: the follow-up of the 92-93 experiment

1997-98 Field Report

Institute for Marine and Atmospheric research Utrecht (IMAU)

Utrecht University

# Meteorological and glaciological investigations on a blue ice area in the Heimefrontfjella, Dronning Maud Land, Antarctica: the follow-up of the 92-93 experiment

1997-98 Field Report

June 1998

R. Bintanja, C.H. Reijmer, H. Snellen , M.P.A. Thomassen

*Institute for Marine and Atmospheric research Utrecht (IMAU)*
*Utrecht University*

## Contents



Photo cover: Swedish research station Svea in the Scharffenbergbotnen valley, Dronning Maud Land, Antarctica. In the background are the blue ice area on the valley floor and the icefall.

# 1. Introduction

The present-day state and the temporal changes in the surface mass balance of Antarctica are important issues in the current sea level change debate. To understand more thoroughly the spatial distribution of the surface mass balance and the processes in the atmospheric boundary layer over Antarctica, a meteorological experiment was conducted in the vicinity of a blue ice area (BIA) near the Swedish research station Svea (74° 35' S, 11° 13' W) in the Heimefrontfjella, Dronning Maud Land, Antarctica, during the austral summer 1997-98. BIAs experience net mass loss through sublimation, whereas at the surrounding snow-covered areas net accumulation occurs. This means that the spatial variability in surface mass balance components will be large on a relatively small spatial scale (Bintanja and van den Broeke, 1995a). BIAs are known as the 'ablation islands' of the Antarctic ice sheet (Bintanja, 1998). It is also suggested that the surface area occupied by BIAs may be sensitive to climatic changes, caused by eventual changes in surface energy balance (Bintanja and van den Broeke, 1995c) or horizontal snowdrift transport (Van den Broeke and Bintanja, 1995b). Because of the fact that BIAs have a negative surface mass balance, ice flows towards BIAs where it eventually surfaces. As a result, BIAs provide easy access to old ice for paleoclimatic studies (Van Roijen et al., 1995). Ice drilled in the BIA will be analysed for its age and chemical contents.

The present meteorological experiment can be considered as the follow-up of the 1992-93 experiment to the same area (Bintanja et al., 1993, 1995), which was the first to measure in detail the meteorological conditions over blue ice and to yield blue ice cores for $^{14}C$ dating. After analysing the 1992-93 data, several questions came up regarding the meteorological characteristics of blue ice, the mesoscale circulation in the Heimefrontfjella, and the age-distribution of the blue ice. To increase our knowledge in these matters, new and more extensive meteorological instrumentation was used, measurements were carried out at other locations and two medium-deep ice cores were taken in the blue ice along with three shallow ice cores.

The meteorological experiment comprised seven 'profile' stations, with wind, temperature and humidity sensors at three or five levels, shortwave and longwave radiation measurements and ice/snow temperature measurements. At two sites, direct turbulence measurements were carried out. Upper-air measurements were carried out with a cable-balloon system and a radiosonde system. Additionally, snowdrift, ice-ripple, bi-directional albedo and synoptic observations were performed. As part of the EPICA (European Project of Ice Coring in Antarctica), six automatic weather stations were erected in the western part of Dronning Maud Land. These stations will transmit their data for two years or more, providing insight in the annual cycle of the meteorological conditions in this region. Details of the measuring equipment and procedures, as well as a selection of the first results will be presented.

The ice core drilling was conducted in the blue ice area closest to Svea. Two medium-deep cores were taken (52 and 85 m), which will be used for $^{14}C$ analyses to determine the depth-distribution of the age of the ice. Additionally, three shallow cores were taken. A complete description of the methods, equipment and experiences of the ice drilling activities will be given.

During the expedition, Swedish scientists were involved mainly in radio-echo soundings to infer snow layer and ice depth, medium-deep firn/ice coring near Wasa and on the plateau Amundsenisen (see section 6), chemical analyses on firn from shallow cores and snow pits, GPS surveys of stakes to measure ice velocity, stake mass balance measurements and ice temperature measurements. Finnish scientists performed geological and geodetic research in the Vestfjella and Heimefrontfjella region.

*Figure 1. Location of the Vestfjella and Heimefrontfjella mountain ranges in western Dronning Maud Land, Antarctica, where the Swedish research stations Wasa and Svea are situated.*

## 2. Logistics

Norway, Sweden and Finland take turns in organising a NARP (Nordic Antarctic Research Programme) expedition to Dronning Maud Land, Antarctica. In 1997-98 it was Sweden's turn to organise the logistics. SWEDARP (Swedish Antarctic Research Programme) chose to co-operate with South-Africa to organise their Antarctic activities for 1997-98, and two South-African ships (Outeniqua and Agulhas) were consequently used for transports of goods and people to the Antarctic. The Dutch party was on the Outeniqua only. On the Antarctic continent, transport was by track vehicle, helicopter and snow scooter. The SWEDARP party consisted of 17 persons (including four Dutch). The Swedes employ two stations in Dronning Maud Land, Wasa in the Vestfjella and Svea in the Heimefrontfjella (Fig. 1). Logistic activities concentrated on well-known routes between the ice edge (Rampen), Wasa, Svea and the plateau Amundsenisen. Below follows a time schedule of the most important logistic and research activities during the 1997-98 field season:

| | |
|---|---|
| March 3 - 8, 1997 | training course in Ann, Sweden, with all expedition members |
| March 27 - April 10 | test medium-deep drilling in Sweden |
| April 24 - May 2 | test medium-deep drilling in Svalbard |
| June - September | calibrating and testing of meteorological equipment at the KNMI and at Cabauw, the Netherlands |
| October 16 | departure of equipment to South-Africa |
| November 30 | departure of Dutch party from Amsterdam |
| December 4 | departure of Outeniqua and Agulhas from Cape Town |
| December 14 | Outeniqua arrives at Rampen (72° S, 16° W) |
| December 15 | helicopter transportation of meteorologists to Svea |
| December 23 | arrival of equipment and drilling team at Svea |
| December 25 | start of the first medium-deep blue ice drilling near Svea |
| December 27 | final two meteorological profile stations erected (sites 4 and 5) |
| December 29 | first radiosonde sounding at Svea |
| January 3, 1998 | start of EPICA traverse to Amundsenisen |
| January 4 | first cable-balloon sounding at Svea |
| January 21 | return of EPICA traverse, start of second medium-deep drilling near Svea |
| January 29 | departure of drilling team to Wasa |
| January 31 | Start of medium-deep drilling between Wasa and Fossilryggen |
| February 5 | final day of meteorological experiment |
| February 6 - 9 | packing of meteorological equipment |

| | |
|---|---|
| February 10 | transportation of equipment and meteorologists to Wasa by track vehicle |
| February 14 | transportation of equipment and people to Rampen |
| February 17 | transportation of people and part of the equipment to Outeniqua |
| February 24 - 25 | transportation of the rest of the equipment to Outeniqua |
| March 4 | Outeniqua arrives in Cape Town |
| March 6 | Dutch party arrives in Amsterdam |
| April 21 | meteorological and drilling equipment arrive in Rotterdam, the Netherlands |
| June - July | ice cores arrive in Utrecht, Netherlands |
| May - July | calibrating and testing of meteorological equipment at Cabauw, the Netherlands |

The meteorological equipment at the seven designated sites (see Fig. 2) were visited in different ways. Sites 1, 2 and 3 could be reached easily by snow scooter, which was done at least every 3 days. Site 4 was further away from Svea, and was therefore visited only once by scooter. Site 5 was never visited during the measuring period, but was erected and taken down by scooter. Sites 6 and 7 were erected on December 15 and taken down on February 17 using helicopter, with no visit in between. Travel between Rampen, Wasa, Svea and the plateau Amundsenisen was mainly by track vehicle and 4WD jeeps. Most of the equipment, including a freezing container to store ice cores, was transported by Hägglund track vehicle.

## 3. Meteorological equipment, set up and data acquisition

The meteorological equipment is more or less similar to that used in previous expeditions to the Antarctic, the Alps, and Iceland (Bintanja et al., 1993; Greuell et al., 1995; Oerlemans et al., 1998). Detailed descriptions of various parts of the equipment can be found in these reports.

*Figure 2. (Opposite page) Location of the seven meteorological measuring sites in the central Heimefrontfjella. Altitude contour lines are drawn every 100 m. Light grey and dark grey areas represent exposed rock and moraine, respectively. Adapted from the map Heimefrontfjella Nord (Maudheimvidda), Sheet D8, Norsk Polarinstitutt (Oslo 1988), 1:250 000.*

In this section, we will describe the instrumentation (sensors, dataloggers, mast constructions) used at the several measuring locations. Here follow some characteristics of the seven sites (see also Fig. 2 for the location of the sites). SEB stations measure the surface energy balance in detail (with 5-level profile masts and turbulence measurements), whereas METEO stations perform less detailed measurements (3-level profile mast). The position of each site was determined by GPS. Notice that some of the altitudes given in the table do not coincide with the altitude as indicated in Figure 2, especially with regard to site 7. This is because of inaccuracies of the map.

| Site | Geographical position | Blue ice or Snow | SEB or METEO | Distance to Svea (km) | Altitude (m a.s.l.) |
|---|---|---|---|---|---|
| 1 | 74° 34' 36" S, 11° 03' 07" W | B | SEB | 6.3 | 1180 |
| 2 | 74° 34' 22" S, 11° 08' 17" W | B | METEO | 3.7 | 1210 |
| 3 | 74° 28' 53" S, 11° 31' 01" W | S | SEB | 12.5 | 1170 |
| 4 | 74° 33' 35" S, 11° 57' 50" W | S | METEO | 18.8 | 1115 |
| 5 | 74° 42' 47" S, 11° 50' 38" W | B | METEO | 25.0 | 1310 |
| 6 | 74° 34' 01" S, 10° 42' 44" W | S | METEO | 15.5 | 1665 |
| 7 | 74° 33' 21" S, 09° 24' 14" W | S | METEO | 54.0 | 2100 |

The present site 1 is close to the 1992-93 site 2, while the present site 3 is close to the site 5 in 1992-93.

*Meteorological profile stations*

The instrumentation used at the various sites is given in the following table. Each mast consist of a 4-legged construction standing freely on the surface to which a vertical mast is attached. Horizontal bars are connected to the vertical mast which carry the various sensors. Most mast parts are made of aluminium. Steel cables connect the top of the mast to each leg to ensure a rigid construction and to minimise unwanted vibrations in sensors and mast constructions. Each station typically took one to two hours to erect. Power for each station was provided by batteries which were charged by two solar panels, one on the datalogger box and one attached to the mast construction. All stations worked the entire period (28 December to 5 February), with the exception of sites 4 and 5 which were taken down already on 3 February for logistic reasons. Only minor problems with a few sensors were encountered. On sites with more than one sets of instrumentation, the instrumentation was placed in an array perpendicular to the prevailing wind direction to prevent wind disturbances from one set affecting another. Below follows a summary of the meteorological equipment at each site.

**Site 1** Profile mast with wind speed, temperature, humidity sensors at 5 levels (0.5, 1, 2, 4 and 9 m), wind direction at 2 levels (2 and 9 m), radiation (shortwave and longwave incoming and outgoing) at 1.5 m, and ice temperatures at 5 levels (5, 10, 20, 40, and 80 cm depth below the surface).

Turbulence mast with a sonic fast-response anemometer and a Lyman-□ humidity sensor at 2 m.

Snowdrift sensors at 4 levels (10, 20, 40 and 80 cm above the surface) from 29 December to 25 January.

**Site 2** Profile mast with wind speed, temperature, humidity sensors at 3 levels (1, 2 and 6 m), wind direction at 1 level (6 m), radiation (shortwave and longwave incoming and outgoing) at 1.5 m, and ice temperatures at 5 levels (5, 10, 20, 40, and 80 cm depth below the surface).

**Site 3** Profile mast with wind speed, temperature, humidity sensors at 5 levels (0.5, 1, 2, 4 and 9 m), wind direction at 2 levels (2 and 9 m), radiation (shortwave and longwave incoming and outgoing) at 1.5 m, and snow temperatures at 5 levels (5, 10, 20, 40, and 80 cm depth below the surface).

Turbulence mast with a sonic fast-response anemometer and a Lyman-□ humidity sensor at 2 m.

Snowdrift sensors at 4 levels (10, 20, 40 and 80 cm above the surface) from 25 January to 7 February.

**Site 4** Profile mast with wind speed, temperature, humidity sensors at 3 levels (1, 2 and 6 m), wind direction at 1 level (6 m), radiation (shortwave and longwave incoming and outgoing) at 1.5 m, and snow temperatures at 5 levels (5, 10, 20, 40, and 80 cm depth below the surface).

**Site 5** Profile mast with wind speed, temperature, humidity sensors at 3 levels (1, 2 and 6 m), wind direction at 1 level (6 m), radiation (shortwave and longwave incoming and outgoing) at 1.5 m, and ice temperatures at 5 levels (5, 10, 20, 40, and 80 cm depth below the surface).

**Site 6** Profile mast with wind speed, temperature, humidity sensors at 3 levels (1, 2 and 6 m), wind direction at 1 level (6 m), radiation (shortwave and longwave incoming and outgoing) at 1.5 m, and snow temperatures at 5 levels (5, 10, 20, 40, and 80 cm depth below the surface).

**Site 7** Profile mast with wind speed, temperature, humidity sensors at 3 levels (1, 2 and 6 m), wind direction at 1 level (6 m), radiation (shortwave and longwave incoming and outgoing) at 1.5 m, and snow temperatures at 5 levels (5, 10, 20, 40, and 80 cm depth below the surface).

All Vaisala temperature/humidity sensors were ventilated. Only the ventilation of the Vaisala sensors at site 7 appeared to have stopped somewhere during the measuring period presumably because of the low temperatures at this high-elevation site. Some minor electronic problems were encountered with a few Aanderaa wind speed sensors. Melt water in cables caused some problems with the Kipp CNR1 sensor at site 2. Specifications of all sensors used in the profile stations are given in the two tables below.

| Sensor | Type | Range | Sites | Precision |
|---|---|---|---|---|
| Air temperature | Vaisala HMP35AC | -55 to +49 °C | 1 - 7 | 0.2 °C |
| Humidity | Vaisala HMP35 AC/D probe | 0 to 100% | 1 - 7 | 2% (RH < 90%)<br>3% (RH > 90%) |
| Wind speed | Vector A100R | 0.2 to 60 m $s^{-1}$ | 1, 3 | 0.1 m $s^{-1}$ |
| Wind speed | Aanderaa 2740 | 0.2 to 60 m $s^{-1}$ | 2, 4, 5, 6, 7 | 0.2 m $s^{-1}$ or 2% |
| Wind direction | Vector W200P | 0 to 360 deg. | 1, 3 | 2 deg. |
| Wind direction | Aanderaa 3150 | 0 to 360 deg. | 2, 4, 5, 6, 7 | 5 deg. |
| Ice/snow temp. | Campbell 107 temp. probes | -40 to +56 °C | 1 - 7 | 0.2 °C |

| Sensor | Type | Spectral range | Sites | Precision |
|---|---|---|---|---|
| Pyranometer | Kipp CNR1 SW | 305 to 2800 nm | 2, 6, 7 | 2% |
| Pyrradiometer | Kipp CNR1 LW | 5000 to 50000 nm | 2, 6, 7 | 15 W $m^{-2}$ |
| Pyranometer | Kipp CM14 | 305 to 2800 nm | 1, 3, 4, 5 | 2% |
| Pyrradiometer | Eppley PIR2 | ± 3000 to 60000 nm | 1, 3, 4, 5 | 10 W $m^{-2}$ |

Sensors at the profile stations sampled every 2 minutes (except the stations at sites 6 and 7, which sampled every 5 minutes), after which the data was stored automatically on a memory card. Sites 1, 2 and 3 were visited every three days, when data cards were exchanged and the data was copied and stored onto a computer at the base. After that, calibration coefficients were applied, and 30-minute, hourly, and daily averages calculated which are then ready for analyses. Simultaneously, simple surface energy balance calculations were performed, of which the results are presented in section 4.

During three months of testing at Cabauw, the Netherlands, some inaccuracies in the temperature and humidity sensors were apparent from the fairly large differences between the values produced by some sensors. All Vaisala temperature/humidity sensors were baselined against one of the sensors; this sensor was accurately calibrated at the Royal Netherlands Meteorological Institute (KNMI). Because of the large differences, we decided to perform a comparison experiment with the temperature and humidity sensors of the two most important profile masts, those of sites 1 and 3. During the period 17 to 23 December, all ten Vaisala temperature/humidity sensors of these two stations were placed close together near Svea at the same height above the surface (2 m) near Svea. The differences were smaller than those encountered earlier in the Netherlands (probably because of the drier conditions), but were still non-negligible. Therefore, the calibration coefficients were adjusted in such a way to minimise the inter-sensor differences, since we are interested mainly in the differences in temperature and humidity between two (or more) levels to accurately calculate the turbulent fluxes rather than the absolute values of temperature and humidity.

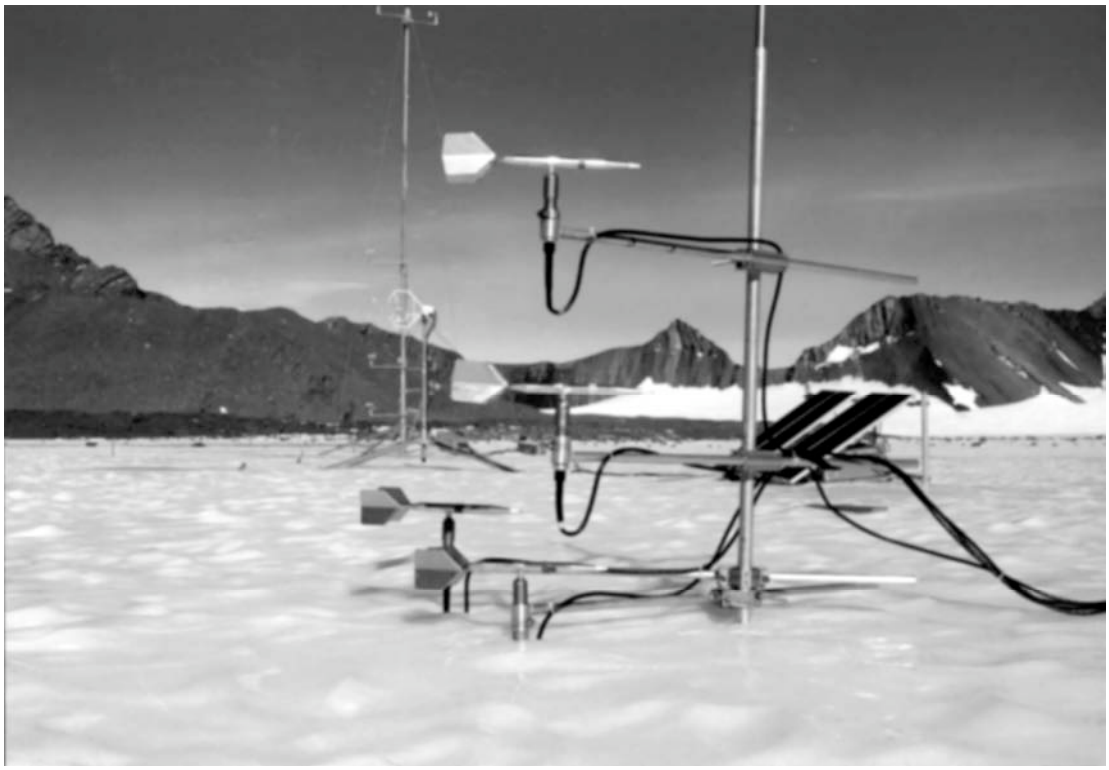

*Figure 3. Picture of the meteorological equipment at site 1. In the front is the snowdrift equipment and in the background are the turbulence station with the sonic anemometer and the 9 m profile station.*

*Turbulence measurements*

Direct turbulence measurements were performed using fast-response anemometers, thermometers and hygrometers. For wind we used sonic anemometers which have a 10 cm vertical measuring path, and measure the three orthogonal wind components and the speed of sound. The instruments were placed at 2 m above the surface. To minimise wind disturbances from the instruments themselves and the mast constructions, the orientation of the instruments was chosen so that they faced the direction of the predominant winds (easterly). The instruments were mounted on a aluminium four-legged mast construction similar to that of a profile station, with steel cables connecting the top of the construction with each leg to prevent unwanted vibrations of the sensors. An unventilated thermocouple was placed close to the sonic measuring path to measure temperature fluctuations. These temperatures can be compared to the temperature calculated from speed of sound measured by the sonic anemometer. More information about technical aspects of the sonic anemometer can be found in the reports of Struijk (1996) and Van de Avoird (1997). The Lyman-□ hygrometers that were used to measure humidity fluctuations were placed at about 30 cm distance to the sonic anemometer at the same height. The moisture range measured by the Lyman-□ can be adjusted by changing the path-length of the radiation between the source and detector tubes. Since moisture contents in the cold Antarctic environment are usually low, we used the maximum distance of 3.5 cm between the source and detector tubes. The tubes have a guaranteed lifetime of 1000 hours or more and were not replaced during the

expedition. Because of the clean environment, the windows of the Lyman-α were cleaned with alcohol only every 2 - 3 weeks. Some specifications of the sensors used in the turbulence masts are given in the following table.

| Sensor | Type | Range | Site | Resolution |
|---|---|---|---|---|
| Sonic anemometer | Campbell CSAT3-3D | u: 0 - 32 m $s^{-1}$ | 1, 3 | u, v: 1 mm $s^{-1}$ |
| | | v: 0 - 64 m $s^{-1}$ | | w: 0.5 mm $s^{-1}$ |
| | | w: 0 - 8 m $s^{-1}$ | | c: 1 mm $s^{-1}$ |
| Thermocouple | Chromel-constantan 75 μm | -40 to 40 °C | 1, 3 | 0.01 °C |
| Lyman-α | KOH-3 | 0.4 - 1.8 g $kg^{-1}$ | 1, 3 | < 0.2% |

The orthogonal wind components u, v and w are the two horizontal wind speeds and the vertical wind speed, respectively, and c is the speed of sound. The resolution in the speed of sound implies a resolution of the air temperature of 0.002 °C. Unfortunately, information about the precision of the various sensors is not provided by the manufacturers.

The sampling frequency was chosen to be 20 Hz to include most of the energy present in turbulent fluctuations. Every three days, 80 Mb of data was produced by each turbulence station, which was stored on a data card. All sensors worked fine during the entire measuring period (28 December to 5 February). Inaccurate readings were caused mainly by snowdrifting particles crossing the measuring paths, which in Antarctica is an unavoidable source of error. Power was provided by batteries which were charged by four solar panels. The solar panels, datalogger and battery box were mounted on a separate construction placed in such a way to minimise disturbance of the wind field.

Testing of the turbulence measuring devices was also carried out at Cabauw, the Netherlands, during summer 1997. Even though moisture (water drops) was occasionally a significant source of error, a useful comparison could be made between the two turbulence stations. This, and a comparison with profile station data, indicated that the instrumentation performed satisfactory. Fluxes and spectra of the two stations compared very well and average wind speed and temperature compared well with those measured by the profile stations. The Lyman-α hygrometers were calibrated at the KNMI before the expedition to determine their response curves. Comparison of average humidity measured by the Lyman-α with that measured by the profile station was hindered by very wet conditions, but in the Antarctic these compared very well.

*Detailed albedo measurements*

Detailed spectral albedo measurements were carried out with three different types of instruments. One experiment was to compare narrow band to broad band irradiances by using four Landsat Global Radiometers (LGR) (two up and two down), measuring incoming and reflected radiation in two spectral intervals, and a broad band pyranometer (up and down). These were mounted horizontally on a rigid construction at about 1.25 m above the surface and were sampled every 2 minutes. This instrumentation was placed over a uniform stretch of blue ice near meteorological site 2 for 23 days and over a flat snow field near Svea for 13 days, yielding a nearly continuous dataset of about 36 days. The spectral range of the LGRs and the Landsat Direct Radiometers (LDRs) was chosen to match channels 2 and 4 of the Landsat-5 Thematic Mapper (TM) multispectral scanner.

The table below lists the characteristics of the various instruments that were used. The accuracy of the various sensors is given for solar zenith angles less than 60°. The accuracy decreases for larger zenith angles (Knap, 1997). The pyrheliometers were used when the solar zenith angle was slightly under 60° (see section 4.6).

| Sensor | Type | Spectral range (nm) | Accuracy |
|---|---|---|---|
| Pyranometer | Kipp CM14 | 305 to 2800 nm | 2% |
| Pyranometer | Kipp LGR1 LGR2 | 520 to 600 nm (TM2) | 2% |
| Pyranometer | Kipp LGR3 LGR4 | 760 to 900 nm (TM4) | 2% |
| Pyrheliometer | Kipp LDR 1 | 520 to 600 nm (TM2) | 5 - 10% |
| Pyrheliometer | Kipp LDR 4 | 760 to 900 nm (TM4) | 5 - 10% |

The second experiment was carried out with the LDRs near the LGR instrumental site. The pyrheliometers were used to measure the bi-directional albedo of blue ice (21 January) and of snow (24 January) near the pyranometer site. The full opening angle of the LDRs is 5°±0.2°, both LDRs being rigidly connected to each other. The distance between the measured surface and the instruments was about 1.5 m. This distance (and the surface 'seen' by the radiometers) was fixed by connecting a thin synthetic wire between a screw driven in the ice and the LDR sensors. The radiation reflected from the surface was measured for different view zenith angles (the angle between the zenith and the radiometer) (i.e. 15°, 30°, 45°, 60°, 75°) and for different relative azimuth angles from (the angle between the solar principal plane and the vertical plane through the radiometer and the measured surface spot) (i.e. 30°, 60°, 90°, 120°, 150°, 180°). The sample rate of the pyrheliometers was 1 s, and each angle was measured for 30 s. Measuring all 30 angles typically took about 1 hour. The experimental set-up was similar to that used by Knap et al. (1997) and Knap and Reijmer (1997). In fact, the instrumentation was used here to extend the results obtained over mid-latitude glaciers.

*Snowdrift measurements*

The snowdrift measuring device was used in co-operation with the Alfred Wegener Institut in Bremerhaven (Tüg, 1988). Snowdrift transport rates were measured at four levels using an pulse counting device. The sensors are sensitive to the momentum transfer of the snow particles colliding with an exposed surface. The output voltage of each sensor is proportional to the integrated (over time) impact impulses of the snowdrift particles. Using calibration coefficients obtained with sand grains in the laboratory yields the snowdrift transport rates. During 6 min, the number of impact events and the summed impact intensity are recorded for each sensor, from which the average impact intensity can easily be calculated. Each sensor directs its sensitive surface towards the wind by using windvanes. This pulse-counting technique is an alternative snowdrift measuring system for the more widely used snowtraps and optical double-beam light pass systems.

The four sensors were mounted at about 10, 20, 40, and 80 cm above the surface (see Figure 3). From 28 December to 25 January the system operated at site 1 on blue ice, only interrupted for a few days due to battery failure. From 25 January to 6 February, the system was placed at site 3 on snow. According to Tüg (1988), single particle momentum can be measured with an accuracy of 5%. Several potential error sources can be thought of, for instance the non-elastic impact of a snow particle when it breaks up on collision with the sensor. All taken together, it is

estimated that the total error in the resulting average impact intensity (or particle momentum) is 10% (Tüg, 1997, personal communication). Power was provided by batteries which were charged by four solar panels. The solar panels, datalogger and battery box were mounted on a separate construction placed in such a way to minimise disturbance of the wind field.

*Cable balloon measurements*

A cable-balloon system was used near Svea to investigate the structure of the atmospheric boundary layer. It was attempted to perform a sounding every three hour continuously over a day to get insight in the diurnal cycle of the boundary layer variables. Only when surface winds do not exceed 10 m $s^{-1}$ the system can be operated. We succeeded to perform eight soundings per day on 8 days (seven near Svea and one near site 1). The soundings near site 1 were performed to obtain insight in the turbulent structure of the boundary layer over a blue ice area very close to the upwind valley wall. Each sounding typically took 45 minutes to carry out, during which the balloon was taken up to a height of about 800 m above the surface. Some characteristics of the balloon system are:

- Balloon: 12 $m^3$, helium, type Airborne K-65, weight 7.3 kg
- Cable: 2000 m Twaron, weight 1 g $m^{-1}$
- Winch: electrical, 750 Watt
- Sonde: AIR tethersonde with sensors for
  air temperature
  humidity from a carbon hygristor
  wind speed
  wind direction from the orientation of the balloon
  pressure
- ADAS (Atmospheric Data Acquisition System) receiver operating at 404 MHz

The ADAS receives samples every 10 second and sends the data to the base station, were it is stored on a computer. In total, 67 soundings were carried out, 8 of which were near site 1 and the rest near Svea. The accuracy of the measured variables is estimated as follows: temperature 0.3 K, relative humidity 5%, pressure 0.5 hPa, wind speed 0.3 m $s^{-1}$, wind direction 5 degrees.

*Radiosonde observations*

We operated a Vaisala MW15 radiosonde system at Svea to study the atmospheric profiles up to a height of 15 - 20 km. Since this system operates in any weather, this system gives invaluable additional information about atmospheric profiles in the lowest kilometer when the weather is too bad for the cable balloon to be used. We used the Vaisala MW15 rawinsonde set with GPS sondes (Vaisala RS80-18G), which measure temperature, humidity and pressure. Wind speed and direction were determined using the GPS wind-finding system. This GPS wind finding system is essential at latitudes south of 73° S, since conventional wind finding systems (OMEGA and LORAN-C) do not operate there. The sondes are carried by Helium-filled 200 g Totex TA200 meteorological balloons. The Vaisala MW15 directly stores the raw and calculated data (e.g., at standard pressure levels) on computer, which enables a quick glance at ongoing meteorological processes. During the period 29 December to 18 January, radiosonde soundings

were performed twice a day, at 12 and 24 hour GMT. From 19 January to 5 February, only the 24 hour GMT sounding was continued. In total, 60 radiosonde soundings were performed. The measuring range and accuracy of the meteorological quantities measured by the radiosonde system are give below. Values are given by the manufacturer.

| Quantity | Range | Accuracy |
|---|---|---|
| Temperature | -90 to +60 °C | 0.2 °C up to 50 hPa |
| Relative humidity | 0 to 100% | 3% |
| Pressure | 3 to 1060 hPa | 0.5 hPa |
| Wind vector | 0 to 180 m $s^{-1}$ | 0.2 m $s^{-1}$ |

*Ice ripple observations*

To get insight in the spatial variability in the ablation rate of blue ice, detailed ablation observations have been carried out. The blue ice surface consists of ripples, mostly of sinusoidal form and often arranged in a very regular pattern. Since ablation rates are so low (usually a few cm per month during the summer), an accurate measuring technique was needed to infer the changes in surface height during the measuring period. Five sites were chosen on the main blue ice area in Scharffenbergbotnen at which the ripple pattern was found to be fairly regular along a stretch of 2 m. Two of these sites were very close to meteorological sites 1 and 2, respectively. At each site, 2 stakes were drilled into the ice. A horizontal bar with cm-scale was attached to these stakes at a fixed height in a direction perpendicular to the ice ripple crests. At the beginning of the measuring period, the height from the bar to the blue ice surface was measured every 2 cm over a 2 m distance with an estimated accuracy of 0.2 mm. This procedure was repeated halfway (at two sites) and at the end of the measuring period. Additionally, wavelength, wave height, wave orientation observations were carried out at each site.

*Ablation measurements*

At each of the seven meteorological sites, one or more ablation stakes were placed close to the meteorological station. Over blue ice the stakes were mechanically drilled into the ice. At each visit of any site, the height of the stake to the free ice/snow surface was measured. This was done by using a wooden board of approximately 70 cm length with a hole in the middle which fitted exactly over a stake. The board was placed over the stake in two fixed directions perpendicular to each other, after which both readings were averaged to yield an mean stake height with an estimated accuracy of 0.5 mm. A disadvantage of this method is that only the ablation/accumulation rates of the heighest surface elements are recorded. Comparison with the detailed blue ice ablation rates as described above will give insight in the accuracy of this widely used method. At sites 1 and 2 extra stakes were added during the measuring period since surface melting rendered the readings from the first stake unreliable. Measuring the ablation rate over blue ice is important since sublimation is the only mechanism influencing the surface mass balance over blue ice, which means that stake readings provide a check for the sublimation rates calculated from the meteorological data.

*Synoptic observations*

Every three hour during the day (9, 12, 15, 18, 21, and 24 hr GMT) synoptic observations were carried out during the entire measuring period (from 17 December to 7 February). On some days, night-time observations (3 and 6 hr GMT) were additionally performed. Most of the observations were performed at Svea station, but when other activities required our presence elsewhere the observations were performed at that other location. The synoptic observations consist of the type of cloud and the amount (in eights of the sky) of each type of cloud and a general description of the weather. In total, 326 synoptic observations were carried out.

# 4. Preliminary results of meteorological measurements

## 4.1 General meteorological situation

The general idea of this meteorological experiment was to extend our knowledge of the meteorology of Antarctic blue ice areas. The 1992-93 expedition to the same area provided a number of valuable insights in the meteorological conditions over blue ice areas and their surroundings (e.g., Bintanja et al., 1993; Bintanja and van den Broeke, 1995; Van den Broeke and Bintanja, 1995). In particular, the results of 1997-98 experiment should provide more insight in the following issues: 1) the meteorological conditions of the area upwind of a blue ice area, and 2) the differences in the surface energy fluxes between blue ice and snow. The locations of the various measuring sites were chosen accordingly (see Figure 2). Site 1, close to site 2 five years ago, is the location where detailed turbulence measurements over blue ice were carried out. At site 3 (site 5 five years ago) similar turbulence measurements over snow were performed over snow. Sites 6 and 7 are located on the upwind (eastern) side of the main blue ice area in Scharffenbergbotnen, while site 4 is located downwind of the blue ice area. Site 2 was placed on the main blue ice area close to Svea, but closer to the equilibrium line than site 1 to investigate whether there are any detectable spatial differences in meteorological variables within a blue ice area. Site 5, finally, is located over a blue ice area near Bratbergshorten to infer whether or not conditions over the well-studied blue ice area near Svea are representative for other BIAs. This choice of meteorological sites, together with the radiosonde balloon and cable-balloon soundings, enables us to obtain a more complete picture (compared to the 1992-93 expedition) of the mesoscale meteorological conditions in the Heimefrontfjella.

Note that all data presented in this section should be considered preliminary, since intercomparison of the various instruments during 1998 may result in (slight) changes in calibration coefficients. Figure 4 shows daily average values of temperature, relative humidity and wind speed measured at sites 1, 3, 6 and 7, as well as cloud amount observed at Svea. In the beginning of January, air temperatures were quite high with occasional above-zero temperatures in daytime at all sites. At the blue ice area this resulted in extensive surface melting and the formation of meltwater lakes. After 10 January temperatures dropped substantially; the end of the warm period coincides with the storm on 8 - 10 January. Site 1 on blue ice is significantly warmer than site 3 over snow at the same elevation, which is caused mainly by the fact that blue ice is heated more vigorously because of its lower albedo (Bintanja and van den Broeke, 1995). Also the rapid descent of adiabatically warmed air down the upwind valley wall contributes to the higher temperatures over blue ice. Obviously, the high-elevation sites 6 and 7 experience the lowest temperatures throughout the measuring period.

With regard to humidity it is clear that site 1 on blue ice has a significantly lower relative humidity than the snow sites 3, 6 and 7. However, if absolute (specific) humidity is considered (not shown) the differences are not so outspoken; this means that the low relative humidity at site 1 is caused by the warm ambient temperatures. Relative humidity is more variable over blue ice.

Daily mean wind speeds are generally between 2 and 8 m $s^{-1}$ at all sites, except during the storm of 8 - 10 January when daily wind speeds at site 1 reached 17 m $s^{-1}$. The maximum wind speed recorded was 40 m $s^{-1}$ at site 2 (this is a maximum value over a 2 minute period). Interestingly, during the storm wind speeds are strongest over the BIA, whereas during the rest of the period site 1 experienced the lowest wind speeds. Strong winds blow from easterly directions, while weak winds mostly blow from the west, in particular over the BIA (Van den Broeke and Bintanja, 1995). Because of the more variable wind climate over the BIA in Scharffenbergbotnen, site 1 experiences the lowest wind directional constancy.

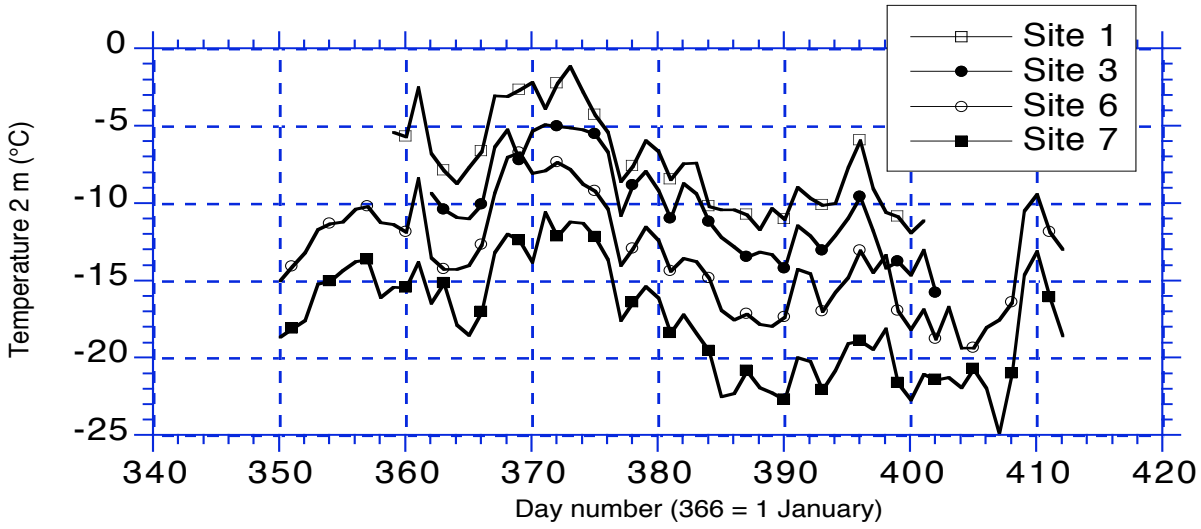


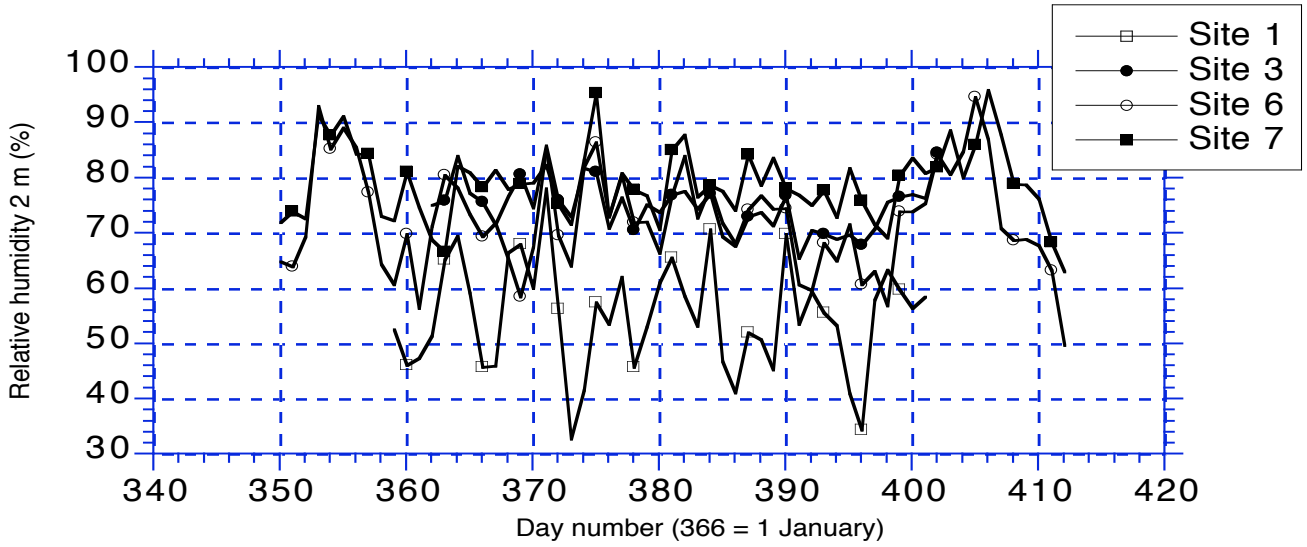

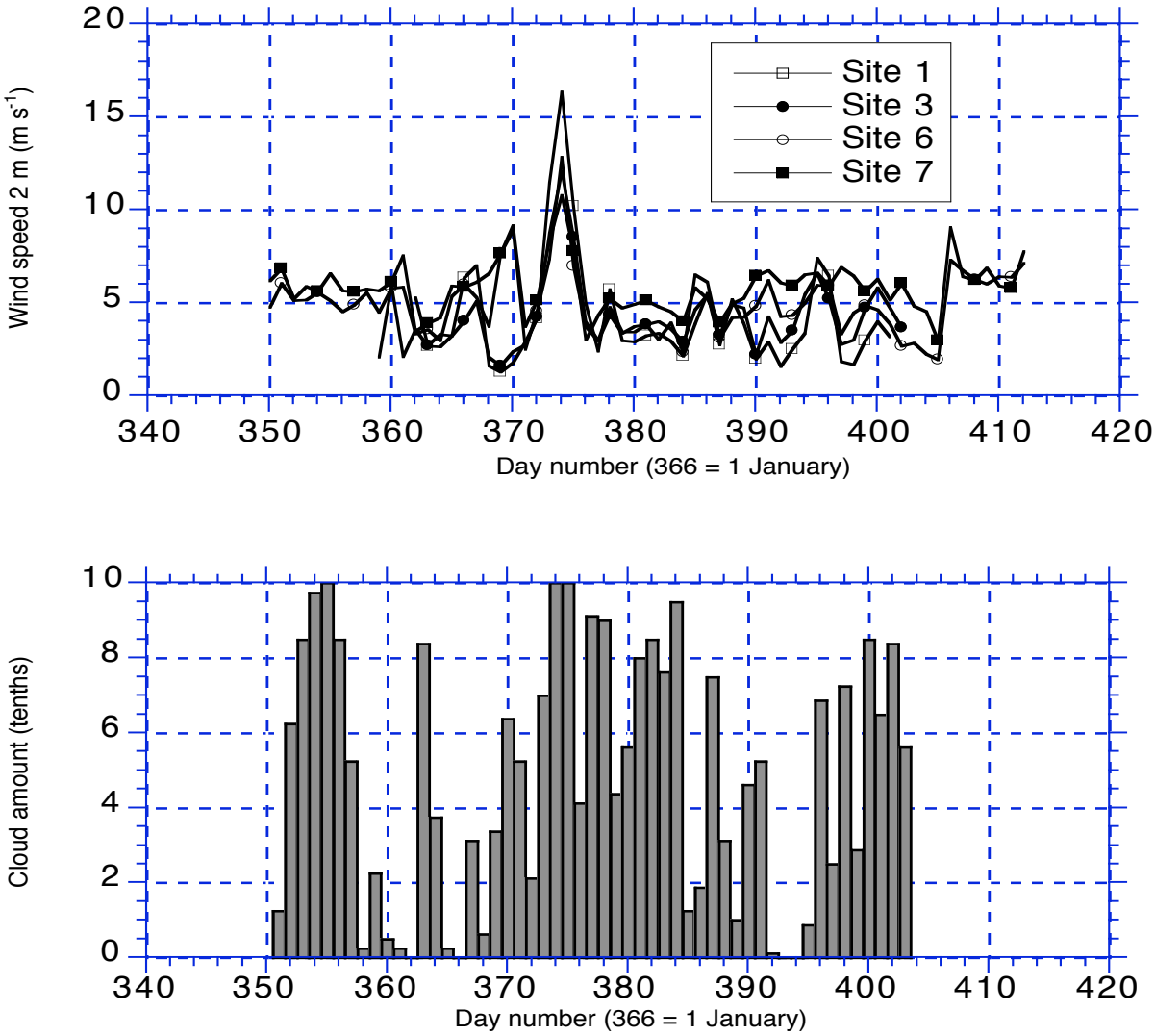


*Figure 4. Variation of daily mean temperature, humidity and wind speed at sites 1, 3, 6 and 7, and daily mean cloud amount at Svea.*

Cloud cover was relatively high, with two main clear periods at the end of December and the end of January. Especially Stratus, Altocumulus and Cirrostratus clouds were commonly observed. Averaged over the entire measuring period, total cloud cover amounts to 3.8 tenths, with the contribution of the low, middle and high clouds being 0.7, 1.6 and 1.6 tenths, respectively.

The following table shows mean values of temperature, relative humidity, wind speed and surface albedo during the period that all stations were operational (28 December to 2 February). The extreme values refer to half-hourly average values. Compared to the summer of 1992-93, the summer temperatures of 1997-98 were about 1 °C warmer (at sites 1 and 3), relative humidities were about the same and wind speeds somewhat lower. Maximum temperatures were above or quite close to 0 °C, resulting in surface melt. It is clear that all blue ice sites (1, 2, and 5) are warmer than the snow sites, as explained above. The difference in temperature between sites 1 and 3 is 2.5 °C, somewhat less than 5 years ago (3.1 °C).

| Site | Temperature (2 m) (°C) | | | Relative humidity (2 m) (%) | | | Wind speed (2 m) (m $s^{-1}$) | | Albedo |
|---|---|---|---|---|---|---|---|---|---|
| | min. | mean | max. | min. | mean | max. | mean | max. | mean |
| 1 | -15.0 | -7.2 | 0.8 | 25.2 | 55.3 | 100.0 | 4.3 | 19.5 | 0.58 |
| 2 | -16.3 | -7.6 | 1.8 | 26.7 | 57.1 | 100.0 | 4.5 | 21.0 | 0.62 |
| 3 | -21.6 | -9.7 | 0.1 | 49.3 | 74.5 | 100.0 | 4.3 | 14.9 | 0.79 |
| 4 | -20.1 | -9.8 | 1.2 | 50.1 | 75.1 | 100.0 | 4.1 | 15.5 | 0.81 |
| 5 | -15.3 | -8.7 | -0.4 | 19.6 | 55.3 | 95.4 | 3.0 | 17.1 | 0.68 |
| 6 | -23.8 | -13.0 | -1.3 | 31.0 | 71.5 | 98.7 | 4.9 | 15.6 | 0.84 |
| 7 | -29.7 | -17.2 | -1.8 | 20.3 | 78.1 | 99.4 | 5.8 | 14.1 | 0.85 |

There is a clear distinction between the relative humidity over blue ice (about 55%) and over snow (about 75%). This reflects the fact that the air over BIAs is warmer and can therefore take up more moisture. In terms of absolute humidity the differences between blue ice and snow are much smaller. Winds are generally strongest on the high-elevation sites 6 and especially 7. However, gusts during the storm are strongest at the blue ice sites, which reflects the highly turbulent character of the boundary layer over blue ice in the lee of nunataks. Five years ago the strongest gusts were also recorded over blue ice (at site 2). The value of the surface albedo obviously differs widely between blue ice and snow. The albedo of blue ice (0.58 - 0.68) seems to be somewhat higher than five years ago. It seems that temporary snow cover was more frequent in the 1997-98 season, and especially at site 5 the blue ice was frequently covered by snow. Over snow, the albedo is relatively constant in time, and ranges from 0.79 to 0.85. Obviously, differences in albedo will cause distinct differences in the surface heat fluxes, as will be demonstrated below.

We will demonstrate the differences in surface energy balance between the various meteorological sites by focusing on a few days in January (8 - 10) during the strong wind period. The strong winds are associated with a deep depression moving eastwards along the coast of Dronning Maud Land. High wind speeds enable a relatively higher accuracy in calculating the turbulent fluxes of sensible and latent heat from the profiles of wind, temperature and humidity by using Monin-Obhukov similarity theory. It must be emphasised that this case study is rather preliminary in view of the sensor intercomparison (and possible calibration adjustments) that has yet to be carried out in summer 1998. Figure 5 displays some meteorological variables and the calculated turbulent fluxes at site 1. Clearly, the peak of the storm occurs at 9 January, when the values of the sensible and latent heat fluxes are maximum. The sensible heat flux is directed towards the surface, indicating a stable stratification in the surface layer and strong cooling of the air. This cooling of the air near the surface over sloping terrain is typical for a well-developed katabatic wind system, which may be 'helping' the synoptic pressure gradient in producing the strong winds. The latent heat flux is negative, which means that water vapour is transported away from the surface (e.g. sublimation). Notice that the magnitude of both turbulent fluxes is about the same during the storm, which implies that surface heating/cooling due to the turbulent fluxes is not very large. The stormy winds and the associated high turbulent fluxes interfere with the 'normal' diurnal cycle in the turbulent fluxes, which will be shown later on.

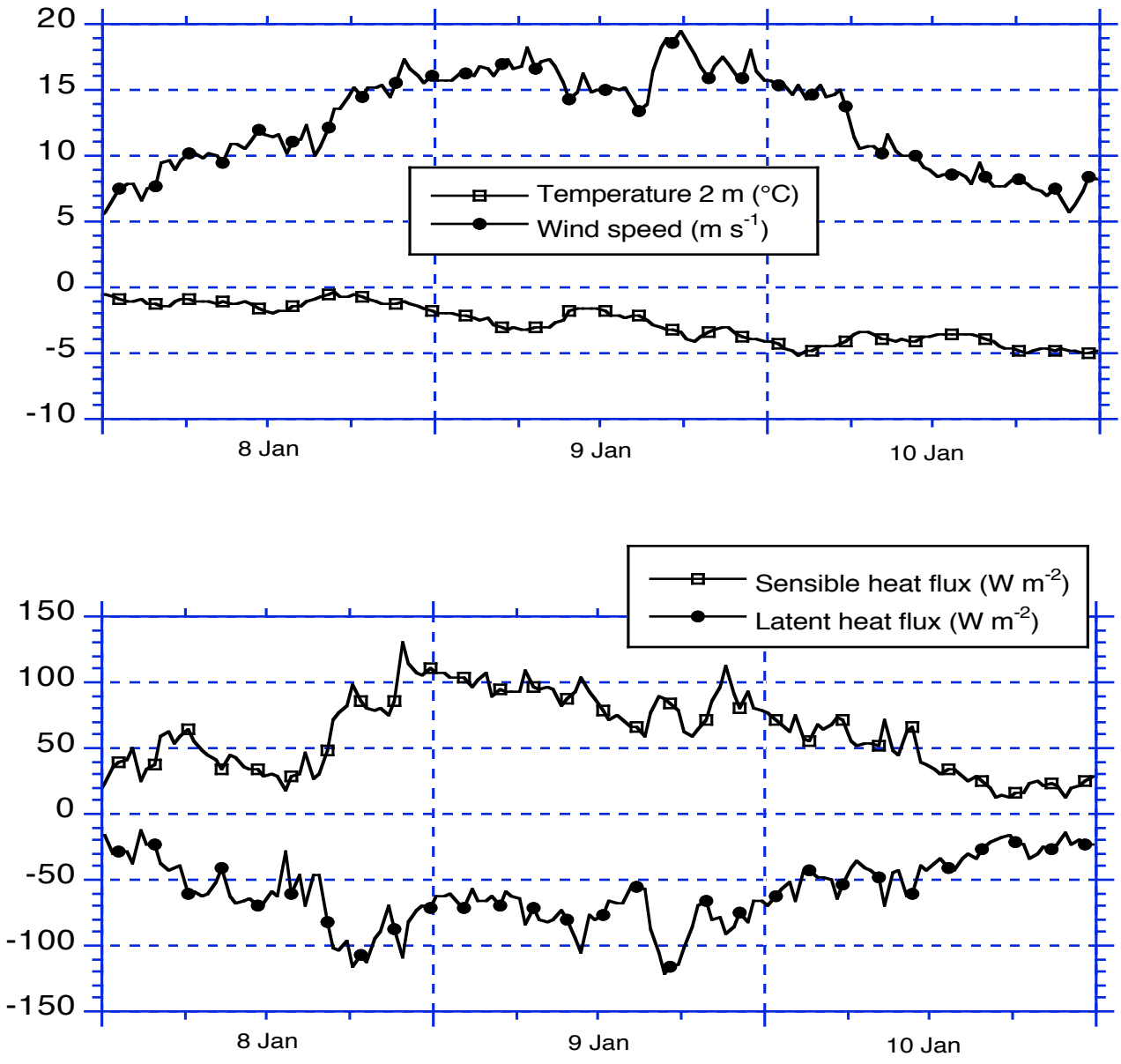


*Figure 5. Variation of temperature, wind speed and the calculated fluxes of sensible and latent heat during the period 8 - 10 January at site 1.*

The table below depicts the mean values of the radiative and turbulent fluxes over the study period (8 - 10 January) for the various sites. (At site 5, wind speed profile measurements were too inaccurate to calculate turbulent fluxes, while at site 2 the longwave radiation sensor gave erroneous readings during this period.) Obviously, the net shortwave flux is highest on the blue ice sites because of their lower albedo. The net longwave flux varies little between the measuring sites. The sensible heat flux is positive everywhere except at site 6. This indicates that cooling of the lowest atmospheric layers occurs on a large scale, and that the katabatic forcing is present

throughout the region. The latent heat flux is negative everywhere, indicating mass loss through sublimation at all locations. Notice that the magnitude of the sublimation rate is quite significant, since a latent heat flux of -32 W $m^{-2}$ is equivalent with a mass loss of 1 mm w.e. per day. Furthermore, the magnitude of the latent heat flux seems to be lower for the high-elevation sites 6 and 7. This can be explained by the fact that the colder the air is, the lower the moisture gradient can be, which implies that latent heat fluxes are smaller (Bintanja et al., 1997). Again, one must bear in mind that the results shown here are very preliminary, as recalibration of sensors (affecting the vertical profiles) may be necessary.

| Site | Type | Net shortwave flux (W $m^{-2}$) | Net longwave flux (W $m^{-2}$) | Sensible heat flux (W $m^{-2}$) | Latent heat flux (W $m^{-2}$) |
|---|---|---|---|---|---|
| 1 | Ice | 94.4 | -45.0 | 61.9 | -59.2 |
| 2 | Ice | 83.0 | – | 32.4 | -80.4 |
| 3 | Snow | 50.4 | -41.7 | 73.6 | -65.1 |
| 4 | Snow | 45.7 | -39.4 | 55.6 | -77.0 |
| 5 | Ice | 77.9 | -51.4 | – | – |
| 6 | Snow | 32.9 | -42.5 | -15.5 | -49.1 |
| 7 | Snow | 41.4 | -46.5 | 43.5 | -12.1 |

### 4.2 Turbulence measurements

At site 1, over blue ice, and at site 3, over snow, direct measurements of surface layer turbulence were performed. The three components of wind speed and the air temperature were measured by a sonic anemometer, while air temperature was also measured using a thermocouple and humidity by means of a fast-response Lyman-□ hygrometer. Sampling took place at 20 Hz, sufficient to capture the contributions of the smallest scales that effectively contribute to the turbulent fluxes. Analyses of the spectra of the various variances and covariances reveals that a slope of -5/3 in the inertial subrange is typical, as expected from theory. This is an indication of the fact that we can have confidence in the turbulence data, even though waves may contribute to the fluxes (in particular at site 1) in the lowest frequency range (Kaimal and Finnigan, 1994). Also, comparison of wind speed, temperature and humidity data from the turbulence sensors with those of the profile stations shows that the temporal variation in these quantities usually agrees very well, as is also often the case for the absolute values.

Figure 6 shows a comparison of the hourly average turbulent fluxes of sensible and latent heat, measured directly and calculated from the measured profiles of wind speed, temperature and humidity at the profile masts using Monin-Obukhov similarity theory. During the night, sensible heat fluxes are positive (downward directed) due to the stable stratification of the atmospheric surface layer caused by longwave cooling of the surface. In daytime the stratification becomes neutral or slightly unstable, a result of the shortwave surface heating. The diurnal cycle of the sensible heat flux agrees very well with that of 1992-93 at the same location (Bintanja and van den Broeke, 1995a). During the night, the flux calculated from profile data is significantly larger than the directly measured flux. At least part of this difference can probably be attributed to errors in the profile measurements, as such errors can give rise to very large errors in the calculated fluxes.

The magnitude of the flux measured by the sonic anemometer compares well with the fluxes of 5 years ago.

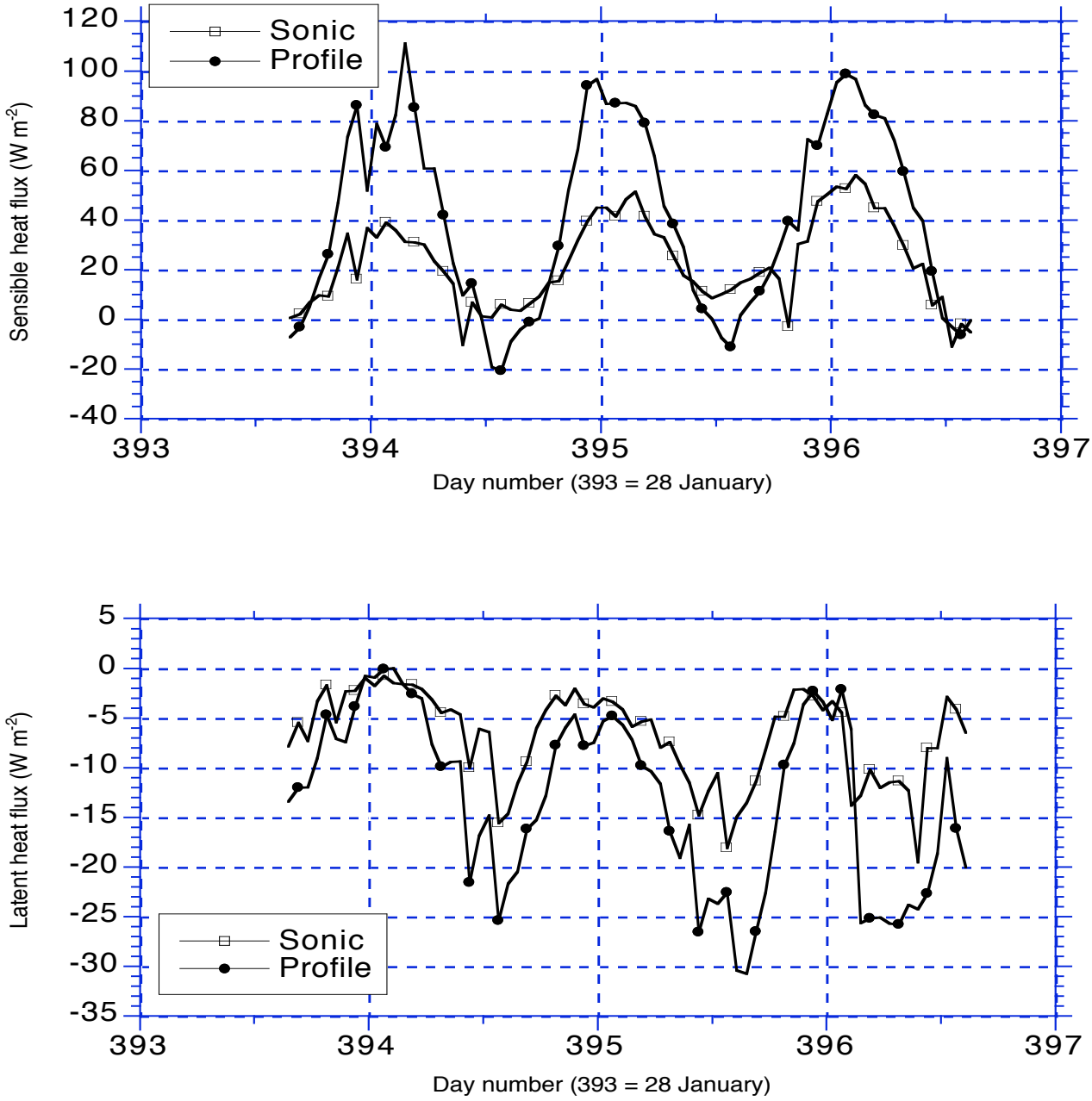


*Figure 6. Comparison of calculated (from profile data) and directly measured sensible and latent heat fluxes over the period 28 - 31 January at site 3.*

The latent heat flux is negative, in particular during the day under neutral or slightly unstable conditions. This indicates that the moisture flux is directed upward. During the night, the moisture gradient becomes very small and sublimation vanishes. This diurnal cycle in latent heat flux

resembles quite closely that of 5 years ago; also the magnitude of the flux agrees well (Bintanja and van den Broeke, 1995a). The agreement between the directly measured latent heat flux and the calculated one is reasonably good, given the uncertainties in the measured humidity profiles. The diurnal cycles of both turbulent fluxes is closely connected to the daily evolution of the boundary layer (e.g. wind speed, temperature distribution), as will be investigated in future studies.

A more accurate examination of the directly measured fluxes will reveal whether standard Monin-Obukhov similarity theory applies over Antarctic snow and ice. In particular over blue ice, values of constants in the stability correction terms may vary from the ones derived from mid-latitude experiments. Another important goal is to use turbulence and profile data to evaluate the roughness lengths over blue ice and snow and compare these with values calculated from the 1992-93 dataset (Bintanja and van den Broeke, 1995b).

### 4.3 Snowdrift measurements

As described in the previous chapter, direct snowdrift observations were carried out over blue ice and over snow by means of an impact-measuring device (Tüg, 1988). The four sensors recorded the 6-minute average drift transport rates (kg $m^{-2}$ $s^{-1}$) of the impacting snow particles. By assuming that snow particles have the same horizontal velocity as the ambient air at the same height, and by extrapolating downward the observed wind profile to the heights of the snowdrift sensors, the vertical profile of suspended snowdrift density (in kg $m^{-3}$) can be calculated. Figure 7 shows a half hourly averages of drift density over snow near site 3 over a 3-day period. Also shown is the extrapolated wind speed at the lowest snowdrift level (8 cm). Wind speeds at 8 cm height higher than about 4 m $s^{-1}$ result in the onset of snowdrifting. Clearly, the onset and cessation of snowdrifting is governed by subtle mechanisms, as small changes in wind speed near the threshold wind speed result in large changes in snowdrift density. An important reason for the large increase in snowdrift density just after the onset of a snowdrift event is the fact that saltating particles regularly bounce with the surface, thereby ejecting other loose particles and increasing the saltating and suspended snowdrift density (e.g. Pomeroy, 1990). An illustrative example is the onset of a snowdrift event in the night of 30 January. While after snowdrift initiation the wind speed remains fairly constant, the amount of snowdrift increases steadily until it peaks around 6 hr. It must be noted that the fetch at site 3 is quite uniform for several tenths of kilometers.

Also interesting to note is that snowdrift density at 18 cm above the surface is about one order-of-magnitude smaller than at 8 cm. Over the lowest 90 cm the decrease is 4 orders-of-magnitude, a vertical profile that agrees well with snowdrift measurements in the Canadian Arctic (Pomeroy, 1992). Further studies will focus on the relation between snowdrift density and wind speed (actually, the dependence of the threshold wind speed on various parameters), the decrease of snowdrift density with height, and the differences in snowdrift quantities and mechanisms between blue ice and snow.

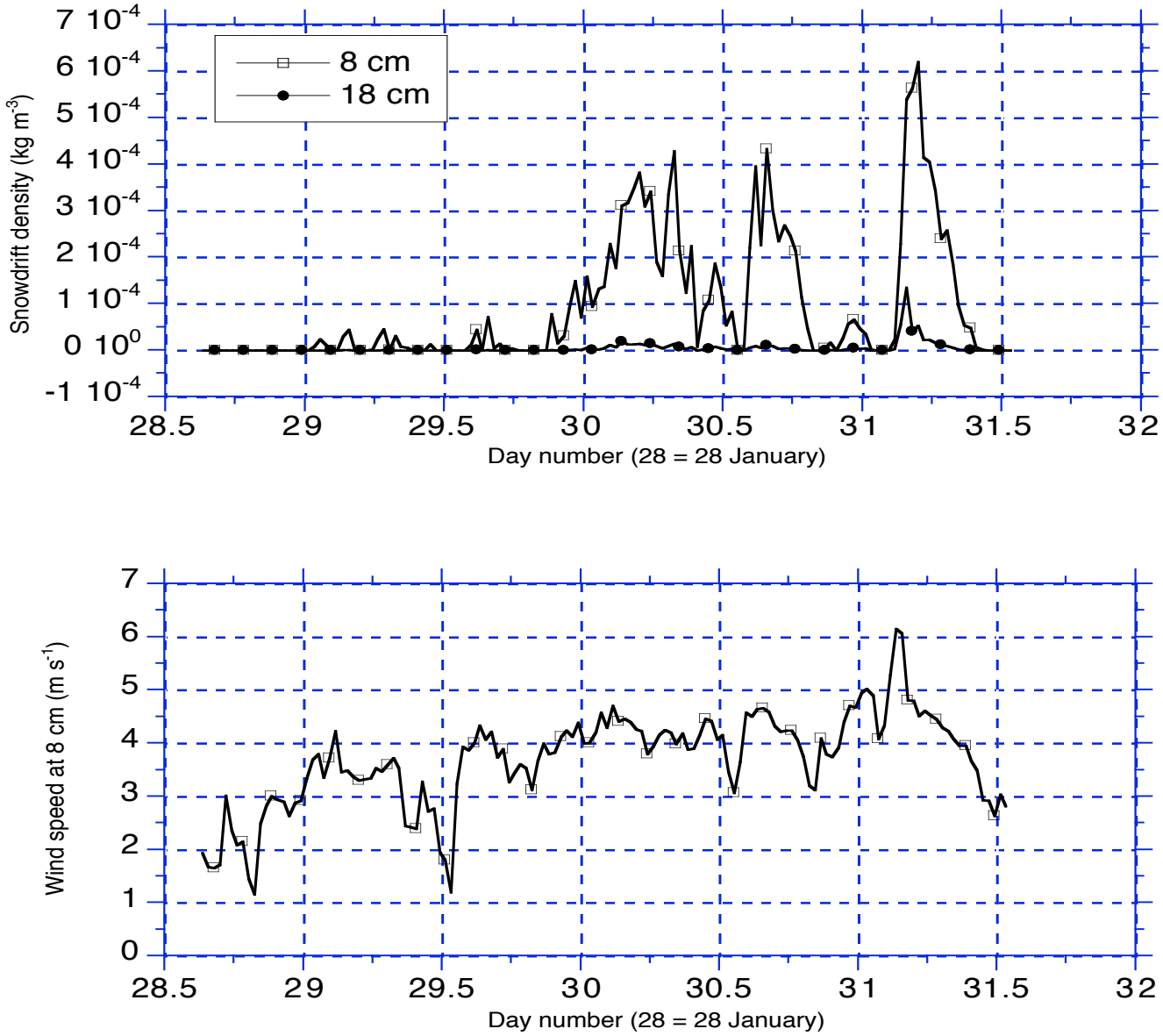


*Figure 7. Half-hourly values of snowdrift density at 8 and 18 cm above the surface and wind speed at 8 cm above the surface at site 3. The wind speed at 8 cm is obtained by extrapolating downward the measured wind speeds at 0.5 and 1 m logarithmically.*

Differences in snowdrift transport rates between blue ice and snow are also of interest with regard to the formation mechanism of blue ice areas. It is suggested (Van den Broeke and Bintanja, 1995b) that the local divergence of snowdrift transport plays an important role in the formation and maintenance of BIAs on the lee side of mountains. Once formed, the smooth surface of BIAs tends to hamper snow accumulation onto the blue ice, since the gusty winds will easily erode the ice surface. It is hoped that the snowdrift dataset can help to explain to what extent these mechanisms are important with regard to the maintenance of BIAs.

### 4.4 Boundary layer structure from cable balloon soundings

The vertical structure of the atmospheric boundary layer was measured with a cable balloon system. During 7 days, every 3 hours a sounding was performed near Svea. During one day, soundings were performed at site 1. Site 1 is located close to the upwind valley wall, which generates strong turbulent motions in the boundary layer near site 1. To illustrate this, Figure 8 shows the variation of pressure (height) with elapsed time of a sounding for a typical ascent at Svea and at site 1. During these soundings, winds were predominantly from easterly directions, that is, from the upwind valley wall. Obviously, near site 1 the balloon experiences much more variations in height than near Svea, culminating in a nearly 30 hPa pressure increase (about 240□m) within a few minutes at its highest level. This irregular behaviour is a clear indication of the vigorous turbulence in the form of waves and eddies in the boundary layer over site 1. Interestingly, the vertical movements of the balloon were most intense at the level of the upwind valley wall crest, which rises 300 - 400 m above the valley floor. Near Svea, soundings were typically very regular, indicating that the turbulence generated by the upwind valley wall has significantly weakened after 6 km. Moreover, the variance of the vertical wind speed profile is much higher for soundings near site 1 than for the soundings near Svea. The presence of topographic-induced turbulence has a pronounced influence on the turbulent structure of the boundary layer over BIAs, and will therefore significantly affect the vertical turbulent transports of momentum, heat and moisture.

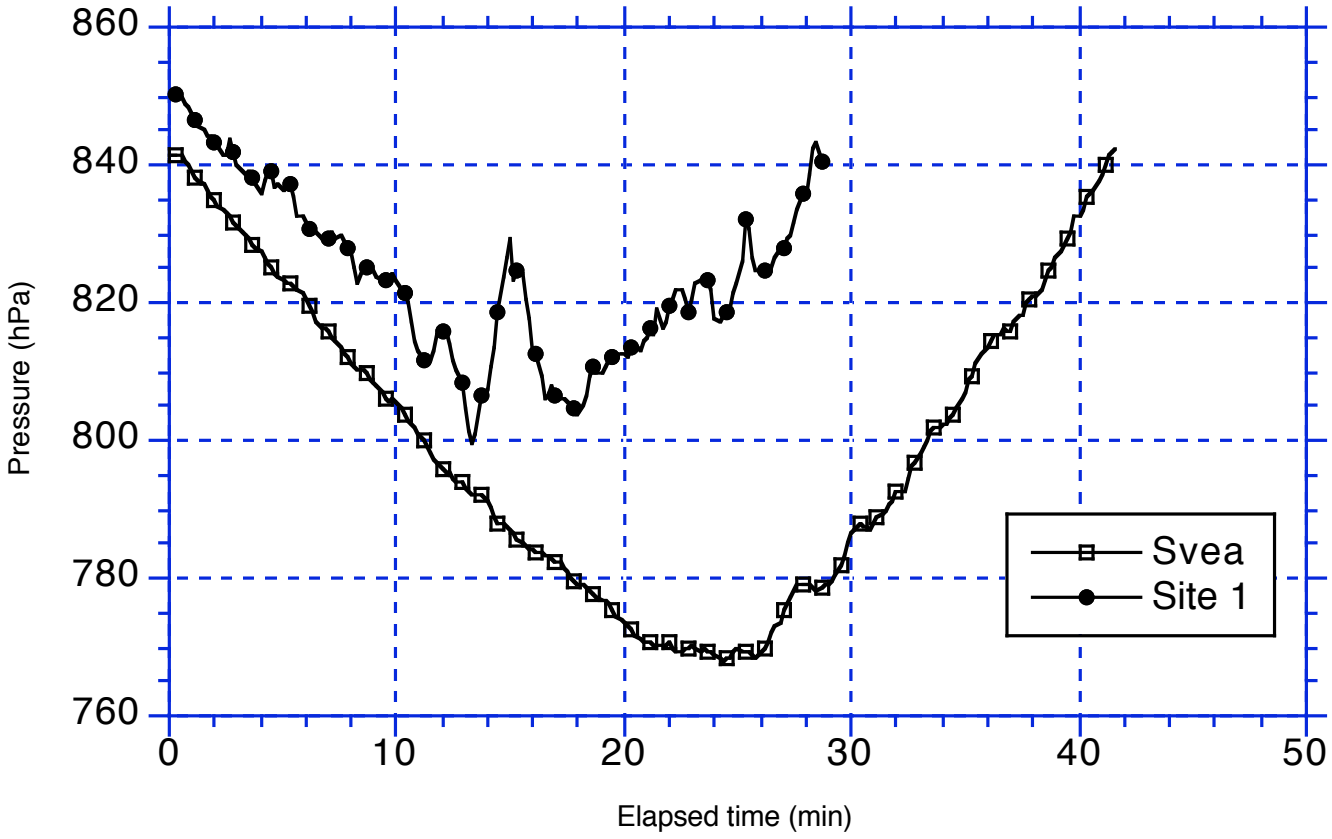

*Figure 8. Typical temporal variation in pressure during soundings over blue ice (site 1) and near Svea, taken at 26 and 16 January, respectively, at 12 hr GMT. Short-term variations in recorded air pressure indicate rapid vertical movements of the balloon.*

The temperature readings from the balloon soundings at 12 hr show that the boundary layer is almost neutrally stratified at both sites, conditions being slightly more stable near Svea. This indicates well-mixed conditions in daytime caused by radiational heating of the surface (Van den Broeke and Bintanja, 1995a). This enables entrainment of free-atmosphere air into the boundary layer. During the night, a shallow stable layer forms near the surface due to radiational cooling, effectively reducing the turbulent mixing between the surface and the atmosphere aloft. The differences between the diurnal cycle of the boundary layer over snow and ice is one of the topics that will be investigated in more detail in the future.

### 4.5 Radiosonde observations

As stated in the previous chapter, radiosonde observations were carried out near Svea first twice a day (12 and 24 hr GMT), Later on once a day (24 hr GMT). As an example, Figure 9 shows the vertical structure of potential temperature and wind speed during the early stages of the storm on 8 January, 24 hr GMT. The stormy period is caused by a low-pressure system moving in easterly directions along the coast of Dronning Maud Land. The lowest 500 m of the atmosphere is very well mixed, as indicated by the near-neutral stratification. Also in the free atmosphere a number of fairly well-mixed layers occur, separated by shallow layers with a very stable stratification. These coincide with the levels of small wind speed gradients, which clearly inhibit vertical mixing. The winds are strongest in the lowest 2 km of the atmosphere, and blow from easterly to north-easterly directions. The wind turns to north-westerly direction in the upper troposphere. The fact that the strongest winds occur in the lowest 1 - 2 km may indicate that near the surface the katabatic forcing helps to accelerate the winds. Near the surface, the wind is more aligned with the regional fall line, as can be expected in case of (partial) katabatic forcing. As shown in section 4.1, cooling of the lowest atmospheric layers is present throughout the region, which is a clear signature of the presence of a katabatic forcing of the winds near the surface.

Regularly, the winds in the atmospheric boundary layer are easterly with a maximum wind speed near 500 m, while above the boundary layer the wind blows from the south-west. This reflects the presence of a katabatic layer near the surface in which essentially downslope flow takes place, underlying a large-scale south-westerly flow forced by the synoptic pressure gradient and the geostrophic winds generated by the thermal field. A study of the mechanisms responsible for the observed flow in the troposphere over Svea and surroundings will be performed with the aid of the radiosonde measurements at Svea and Georg-von-Neumayer and Halley stations at the coast.

### 4.6 Detailed surface albedo measurements

The surface albedo is the ratio of reflected and incident shortwave radiation. Usually, in field experiments the albedo is determined only at a few sites and the measurements may not be representative for larger areas. Satellite remote sensing provides a potential to overcome this

problem. In the process of retrieving a surface albedo from satellite data, several assumptions and conversions must be made. Examples of this are the assumption that snow and ice surfaces reflect the incident shortwave radiation isotropically and the conversion of narrow band albedo values to broad band values. To verify these assumptions and conversions ground measurements of narrow and broad band albedo and bi-directional reflectance were carried out over snow and blue ice.

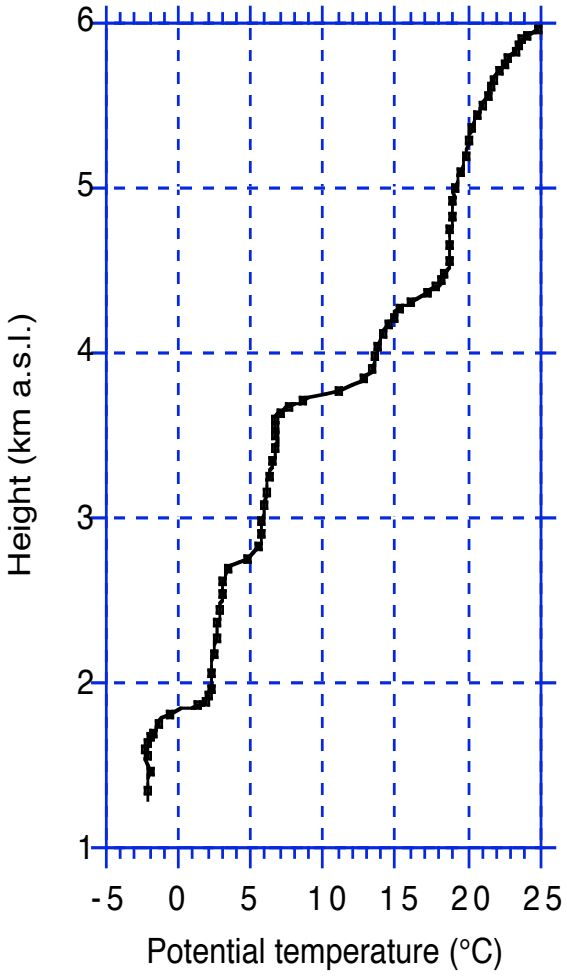
6
5
4
3
2
1
Height (km a.s.l.)
-5
0
5
10
15
20
25
Potential temperature (°C)

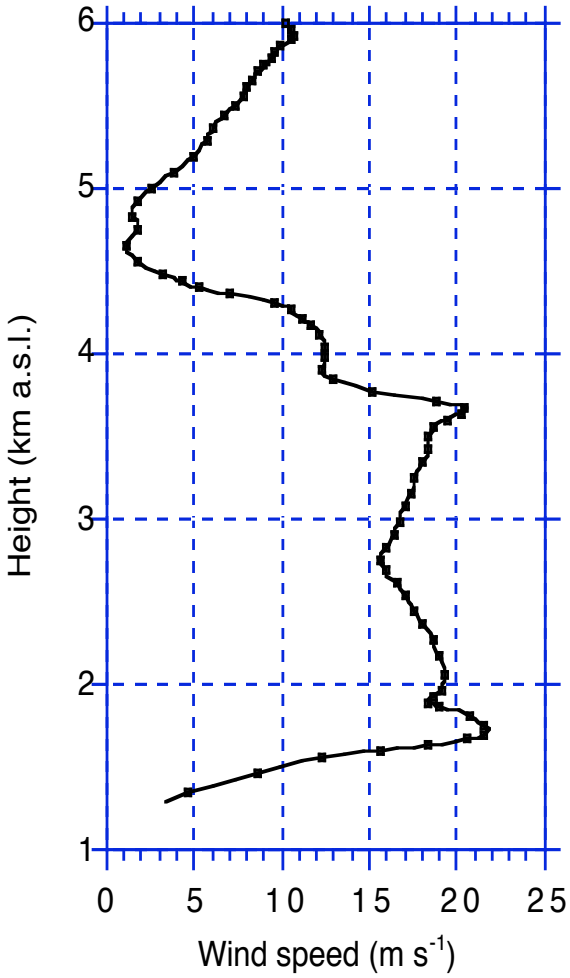


*Figure 9. Vertical profile of potential temperature and wind speed at 8 January, 24 hr GMT as measured with the radiosonde system.*

Using reflectance data obtained over an Alpine glacier, Knap et al. (1997) derived an empirical relationship between the broad band albedo of a glacier surface ($\alpha$) and the narrow band albedos of TM bands 2 ($\alpha_2$) and 4 ($\alpha_4$):

$$\alpha = 0.726\ \alpha_2 - 0.322\ \alpha_2^2 - 0.051\ \alpha_4 + 0.581\ \alpha_4^2$$

The relationship is based on multiple linear regression analysis of simultaneous measurements of the broad band albedo and the albedo in the two TM bands. The ground based instruments used are given in chapter 3 . Figure 10 shows the albedo according to the above equation as a function of the measured broad band albedo. The linear correlation coefficient is reasonable high (0.98), which indicates that the relationship derived at an Alpine glacier may be applicable to Antarctic surfaces as well. This is important, since it seems to be justified to use one equation for all snow and ice surfaces instead of using different equations for each surface type which requires prior knowledge of the type of surface. The distinction between the clusters of low albedo values (blue ice) and high albedo values (snow) is obvious.

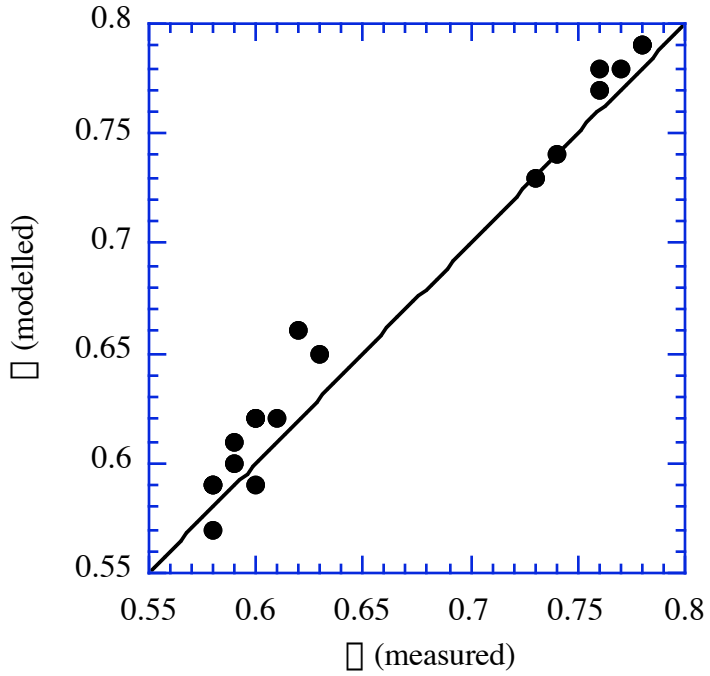


*Figure 10. Modelled albedo versus measured albedo, averaged over fair weather periods with a maximum of 1 day.*

Most natural surfaces do not reflect solar light isotropically (in all directions the same way). A way of expressing the deviation from isotropic reflection is by using the anisotropic reflectance factor f. This factor f is a function of the solar zenith angle $\theta_s$, the view zenith angle $\theta$ and the relative azimuth angle $\phi$, which is defined relative to the solar principal plane (the sun is always in $\phi = 0$). The anisotropic reflectance factor is the ratio of bi-directional reflectance $r(\theta_s, \theta, \phi)$ and the surface albedo $\alpha$: $f(\theta_s, \theta, \phi) = r(\theta_s, \theta, \phi)/\alpha$. To determine $r(\theta_s, \theta, \phi)$, measurements with the Landsat Direct Radiometers (LDR) were done over two surface types, blue ice and snow. The table below gives more details of the measurements (n is number of measured angles).

| Date | n | $\theta_s$ | Surface type | Surface slope | $\alpha$ | View resolution $\theta$ | $\phi$ |
|---|---|---|---|---|---|---|---|
| 21-1-98 | 30 | 55°-56° | Blue ice | 1° | 0.59 | 15° | 30° |
| 24-1-98 | 30 | 56°-60° | Snow | 3° | 0.77 | 15° | 30° |

Figure 11 gives an example of the measured reflection in TM band 2 in the case of $\phi$ = 180° for both surface types. The maximum near $\theta = 60°$ indicates that over blue ice the radiation is reflected almost specular whereas over snow the reflection is more diffuse, a difference that was expected beforehand. For TM channel 4 the reflection characteristics are approximately the same, only the albedo in that channel is lower. A more detailed analysis, including a description of the reflection characteristics at other angles, will be performed using the measurements performed near Svea.

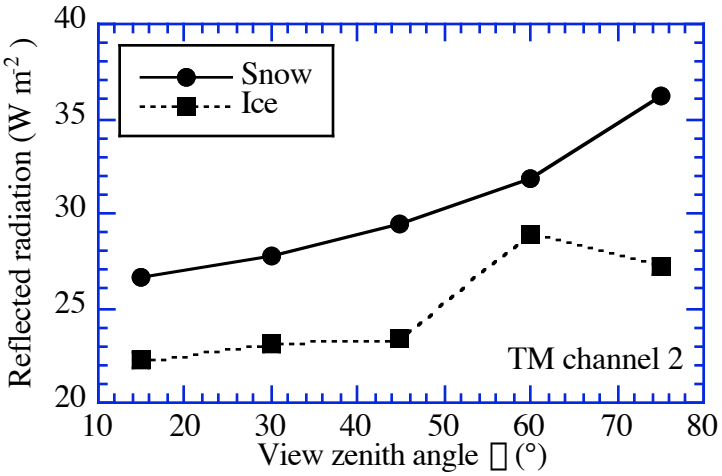


*Figure 11. Reflected radiation in the spectral range of 0.52 - 0.60 μm as a function of the view zenith angle for a solar azimuth angle of 180°.*

### 4.7 Ice-ripple observations

To test whether the structure of the surface elements of blue ice (mostly sinusoidally shaped ripples) can give insight in the sublimation process, detailed observations of the physical dimensions and the temporal evolution of the surface ripples were made. Five sites were chosen with relatively uniform sinusoidal surface ripples, at which the wavelength, wave height, wave form, wave orientation and wave speed were measured. These quantities were measured at the beginning of the measuring period and at the end, while on two sites they were additionally measured halfway.

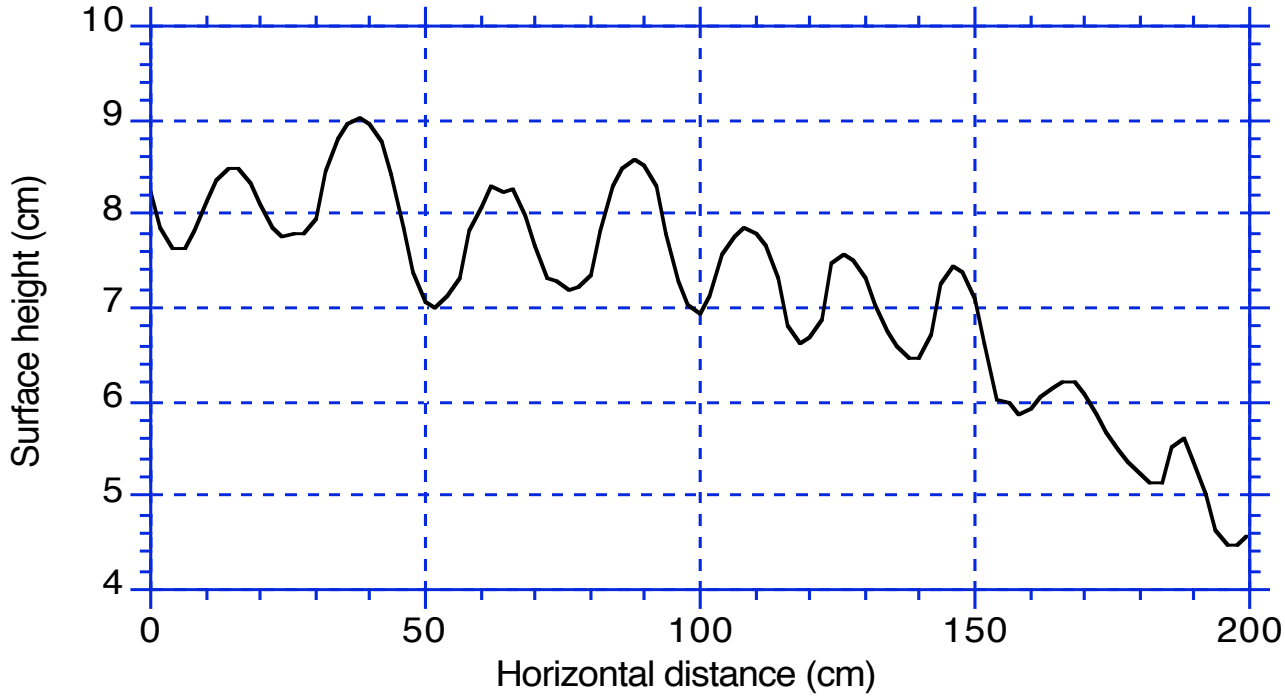


*Figure 12. Cross section of the blue ice surface near meteorological site 2 at 29 December 1997.*

Figure 12 shows a cross-section of the blue ice surface near meteorological site 2. The surface waves are fairly regular, and the average wavelength measures 21.5 ± 3.6 cm and the wave height (through to crest) 1.14 ± 0.40 cm. These figures compare reasonably well with those measured at the other 4 sites, although near site 1 the wave height seems to be somewhat larger. The waves crests and throughs are clearly perpendicular to the prevailing wind at all sites (which in Figure 12 is from the right), which indicates that surface ripple formation must be associated with near-surface turbulence (Bintanja, 1998). Close examination of the cross-section indicates that the lee side of the ripple is somewhat steeper than the upwind side, which is especially clear for the ripples near site 1. Detailed comparison of the cross sections measured at different times will give information on the wave speed and direction. The ultimate goal is to get more insight into the mechanisms governing the sublimation rate of blue ice.

### 4.8. Stake ablation measurements

Stakes were used at every meteorological site to directly measure the surface mass balance during the measuring period. Figure 13 shows the cumulative surface height change at sites 1, 2 and 3. At any of these sites a general decrease in surface height occurs, indicating net ablation. At sites 1 and 2 over blue ice, an increase in surface height was observed in the beginning of January, which is associated with the refreezing of meltwater near the stakes. At that time, new stakes were drilled into the ice at sites unaffected by meltwater. The strong ablation rate at site 3 may indicate high sublimation rates during the warm period. However, at site 3 over snow, the surface mass balance is influenced not only by sublimation but also by precipitation and erosion/deposition of

snowdrift. Nevertheless, the temporal variation in snow height is very smooth and resembles that of sites 1 and 2, suggesting that even over snow sublimation is an important term in the surface mass balance during the measuring period (although it must be remembered that the decrease in water equivalents is smaller over snow because of its lower density compared to blue ice). Mass balance readings from other sites confirm this suggestion. The net mass loss during the measuring period (44 days) is 3.8, 3.3, and 1.7 cm w.e. at sites 1, 2, and 3, respectively. At site 1, ablation is slightly smaller than 5 years ago. Calculations must show how these values compare with calculated and measured latent heat fluxes. Notice that the annual ablation near site 1 is about 12 cm w.e., as independently determined by stake readings (Jonsson, 1992) and analyses of the vertical profiles of $^{14}CO$ and $^{14}CO_2$ in blue ice cores (Van Roijen et al., 1995). At all seven sites, net ablation occurred during the measuring period.

We determined the average sublimation rates from the calculated and measured latent heat fluxes over the period 28 - 31 January at site 3 as shown in section 4.2. Sublimation rates amount to 0.21 and 0.40 mm w.e. $day^{-1}$ for the directly measured and calculated latent heat flux, respectively. Stake readings indicate that the average ablation during this period was 0.58 mm w.e. $day^{-1}$. Since snowdrift did occur regularly during this period (see section 4.3), it can be concluded that snowdrift erosion must have taken place during this period to account for such a high ablation rate. Close examination of the snowdrift data may give more quantitative insight in snowdrift erosion/accumulation.

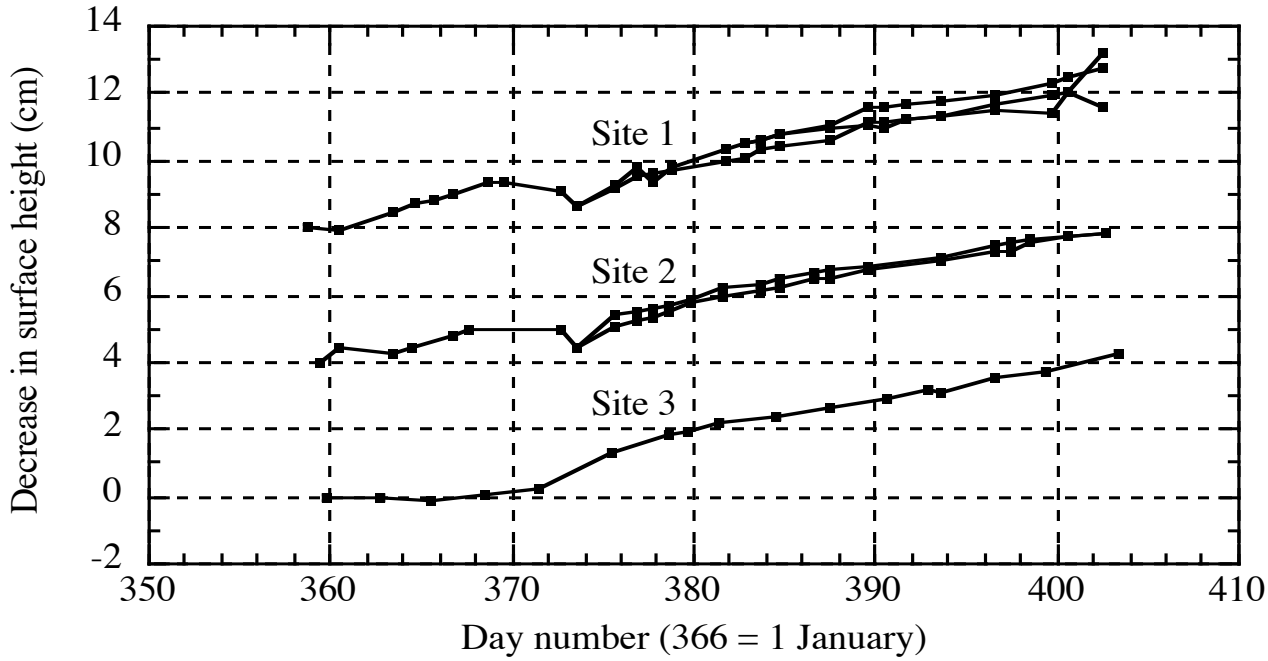


*Figure 13. Cumulative change in surface height at sites 1, 2 and 3 as determined from stake readings. The curves for sites 1 and 2 were offset by 8 and 4 cm for clarity. The different lines at sites 1 and 2 refer to readings from the various stakes at these sites.*

## 5. EPICA automatic weather stations

### 5.1 Instrumentation

In the austral summer of 1997-98, the Institute for Marine and Atmospheric research Utrecht (IMAU), being one of the contributors to EPICA (European Project on Ice Coring in Antarctica), placed six Automatic Weather Stations (AWS) in Dronning Maud land, Antarctica. They were placed on a transect ranging from the coast to the plateau Amundsenisen 600 km inland, along the Swedish research stations Wasa and Svea. The goal of this project is to extend our knowledge of the climatological conditions of this part of Antarctica in order to interpret the results of the deep ice core that will be drilled in this part of the Antarctic ice sheet in the coming years. Another goal is to obtain a better understanding of the spatial and temporal variations in the surface energy and mass balance components of the Antarctic ice sheet. Figure 14 shows the locations of the six weather stations in Dronning Maud Land, Antarctica. Three other IMAU AWSs are located near the Norwegian station Troll, and one on Berkner Island.

The table below provides details of the individual stations, i.e. GPS position, altitude, starting date, surface type and thermistor string depth. All stations were erected by Dutch and Swedish scientists during SWEDARP 1997-98, except from AWS 9 which was erected by scientists from the Alfred Wegener Institute under the supervision of H. Oerter. The site names refer to the internationally accepted names of the various AWS sites.

| | Site | GPS location | Altitude (m a.s.l.) | Starting date | Surface type | Max. string depth (m) |
|---|---|---|---|---|---|---|
| AWS 4 | 1090 | 72° 45' 09" S<br>15° 29' 56" W | 34 | 19-12-97 | Snow | 15 |
| AWS 5 | Camp Maudheimvidda | 73° 06' 19" S<br>13° 09' 53" W | 363 | 02-02-98 | Snow | 100 |
| AWS 6 | Svea Cross | 74° 28' 53" S<br>11° 31' 01" W | 1160 | 14-01-98 | Snow | 15 |
| AWS 7 | SBB 01 | 74° 34' 40" S<br>11° 02' 58" W | 1173 | 31-21-97 | Blue ice | 51 |
| AWS 8 | Camp Victoria | 76° 00' 01" S<br>08° 03' 02" W | 2399 | 12-01-98 | Snow | 100 |
| AWS 9 | DML 05 | 75° 00' 09" S<br>00° 00' 26" E | 2892 | 29-12-97 | Snow | 100 |

*Figure 14. The locations of the six AWSs in western Dronning Maud Land, Antarctica.*

Each AWS consist of a vertical mast with a horizontal bar at approximately 3□n height, which stands on a four-legged frame. Attached to the horizontal bar are the sensors which measure temperature, relative humidity, wind speed, wind direction, snow height, air pressure, shortwave

incoming and outgoing radiation and longwave incoming and outgoing radiation (Figure 15). Note that the Vaisala temperature/humidity sensor is not ventilated because of power supply reasons, which means that in periods with low winds and high insolation these sensors will probably be in error. AWS 7 stands freely on the blue ice surface near meteorological site 1, implying that the height of the sensors above the surface will remain constant. Therefore, the snow/ice height sensor (measuring ablation) of AWS 7 was mounted onto a separate construction that was drilled into the ice. The other AWSs are placed on the snow surface in accumulation areas, where the snow height sensor measures the accumulation rate. These stations will be slowly buried into the snow. All stations are equipped with sufficient batteries to remain working for four years or more. However, the accuracy of the various sensors is expected to decrease significantly after two years of operation. Some characteristics of the various sensors, including their accuracy, is given in the table below.

| Sensor | Type | Range | Accuracy |
|---|---|---|---|
| Wind speed | Young 05103 | 0 to 60 m $s^{-1}$ | 0.3 m $s^{-1}$ |
| Wind direction | Young 05103 | 0 to 360° | 3° |
| Temperature | Vaisala HMP35AC | -80 to +56 °C | 0.3 °C |
| Relative humidity | Vaisala HMP35AC | 0 to 100% | 2% (RH < 90%)<br>3% (RH > 90%) |
| Pressure | Vaisala PTB101B | 600 to 1060 hPa | 4 hPa |
| Short wave radiation | Kipp CNR1 | 305 to 2800 nm | 2% |
| Long wave radiation | Kipp CNR1 | 5000 to 50000 nm | 15 W $m^{-2}$ |
| Snow/ice height | SR50 | 0.5 to 10 m | 0.01 m or 0.4% |

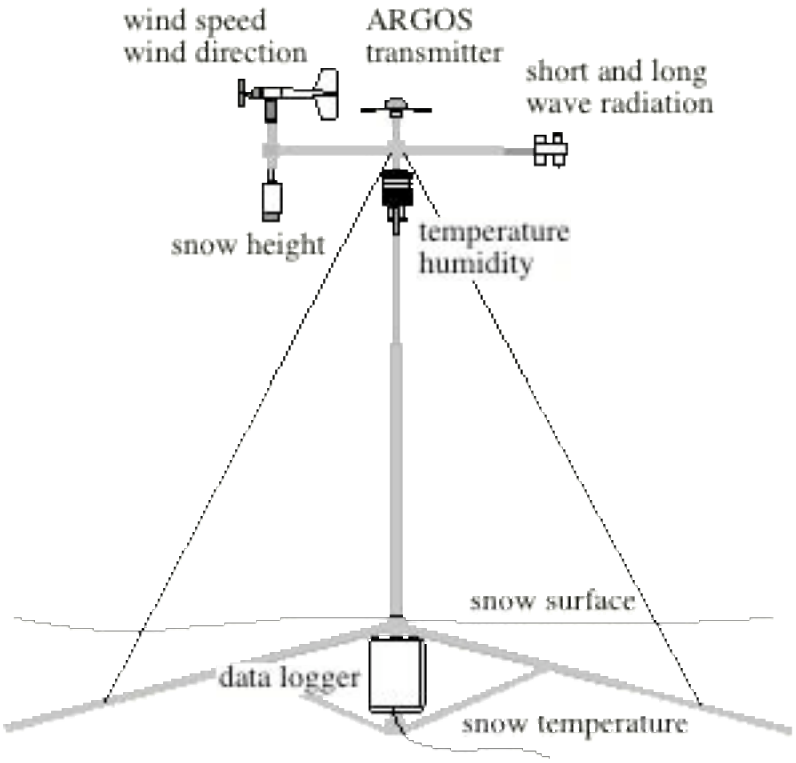

*Figure 15. A schematic illustration of an AWS over snow.*

All six stations were tested during summer 1997 at Cabauw, the Netherlands, at the same test site as the meteorological stations (see section 3). A detailed assessment of the differences between the various AWSs and meteorological stations has yet to be made, but it seems that the agreement between the various sensors was in general favourable. In the Antarctic, two AWSs were close to a detailed meteorological station (AWS 6 near site 3 and AWS 7 near site 1). Comparison of both systems during the summer measurement period (until 5 February) will give additional insight into the accuracy of the AWS measurements. This will be done in the near future.

All stations measure the sub-surface temperatures in the first meter of snow or ice at 5, 10, 20, 40 and 80 cm depth. AWSs 4 and 6 have an additional 15 m string measuring the sub-surface temperatures at 2, 4, 6, 10 and 15 m depth, whereas AWSs 5, 7, 8 and 9 have a 100 m string with sensors at 2, 10, 15, 30 and 100 m. The bore hole near AWS 7 in blue ice is only 51 m deep and therefore the lowest sensor of the 100 m string is at that depth (see chapter 6). Two-hourly means are stored locally in the AWS datalogger and are transmitted every two hours using ARGOS transmitters.

## 5.2 Preliminary results

As an example of the output of the AWSs, Figure 16 shows the temperature development for the six stations from their start (or the first of January) until 15 March. A clear distinction can be seen between the temperature of two high altitude stations 8 and 9 and that of the rest of the AWSs. Interesting is the fact that in some occasions the temperature differences between the lower four stations is small and sometimes even reversed to what one would expect (colder near the coast). This may be due to the fact that AWS 7 is on and AWS 6 near a blue ice area.

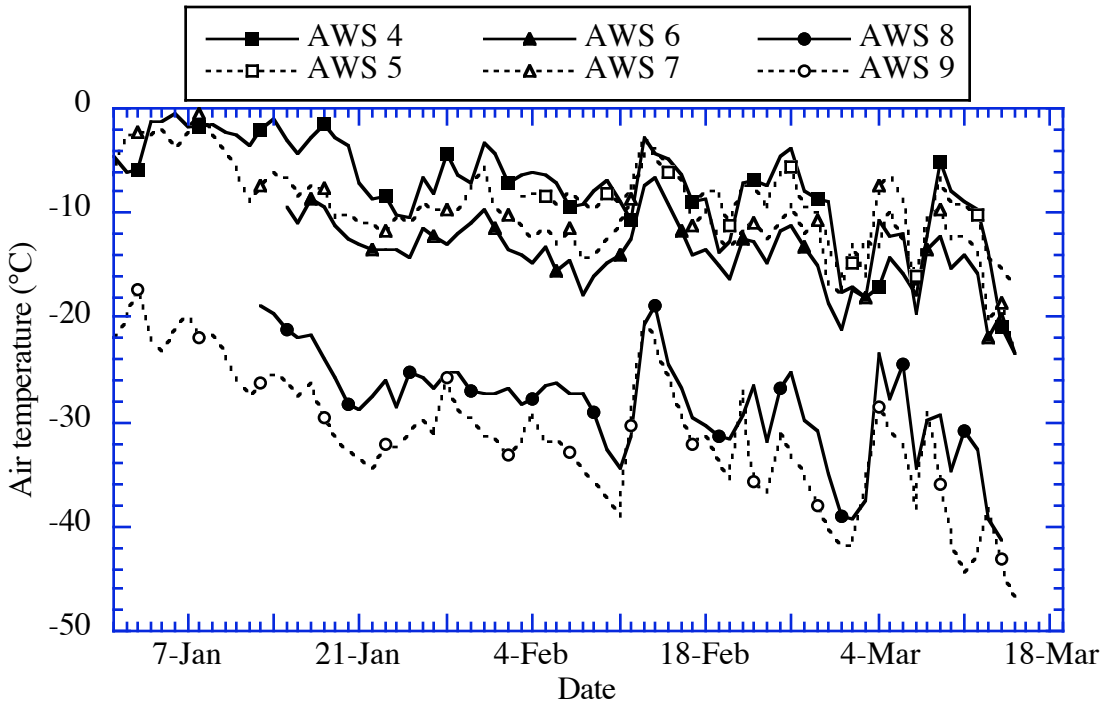

*Figure 16. Temporal variability in air temperature for all the six AWSs from their start (or 1 January 1998) until 15 March 1998.*

More likely, however, is that adiabatic warming of katabatic downflow events and entrainment of warm air into the boundary layer are the main causes for the relatively high temperatures, as AWSs 6 and 7 are located on the steepest part of the ice sheet in this region. On average, higher altitudes imply lower temperatures with the exception of AWS 7, where diabatic radiative heating of the blue ice dominates. Future analyses will provide insight in the prevailing meteorological characteristics in the western part of Dronning Maud Land, for instance in the apparent periodicity in the various meteorological variables as described by Jonsson (1995).

The AWSs additionally measure snow and ice temperatures and various levels. At 10 m depth the amplitude of the annual surface temperature wave is reduced to approximately 5% of its surface value. The 10 m temperature is therefore a reasonable measure of the annual mean surface temperature. Figure 17 shows the absolute and potential 10 m temperature as a function of the distance to the coast for the EPICA transect along the stations Wasa and Svea. The maximum in the potential temperature is associated with a katabatic wind regime (Van den Broeke et al., 1998). At the edge of the plateau where the surface slope is largest (at 200 - 300 km from the coast), stronger katabatic winds enhance downward mixing of relatively warm air into the boundary layer. The higher 10 m temperature of AWS 7 compared to AWS 6 or 8 is explained by the position of the station in a valley on a blue ice area (Bintanja and Van den Broeke, 1995a). There, the lower albedo of the BIA causes diabatic warming and higher potential temperatures compared to its snow covered surroundings.

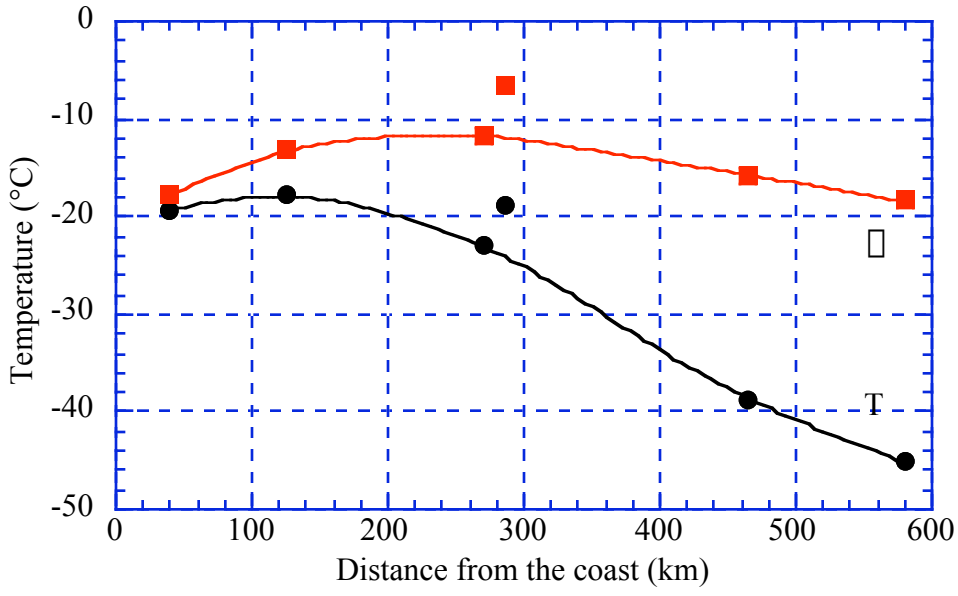


*Figure 17. Absolute (T) and potential temperature ( ) at 10 m depth as a function of the distance to the coast. From left to right are the values of AWS 4 to 9.*

## 6. Ice Coring equipment and methods

The glaciological part of this experiment was, like the meteorological part, a follow up of the 92-93 expedition. In that season, a total of 16 shallow cores (14 cores of 3 meters and two cores of 10 meters) were drilled along two transects in the blue ice (see figure 18). The main goal of this expedition was to obtain two medium long ice cores (100 meters each). The locations for these cores were based on the results from 1992-93. Some background information on the glaciological experiment will be given in the next section.

## 6.1 Objectives

The main objective of the 1992-93 expedition was to study the possibility to use $^{14}C$ (half-life 5730 yr) to date Antarctic blue ice and calculate the specific mass balance (Van Roijen, 1996). Three methods are currently in use for dating ice cores: counting of year layers (only in accumulation areas), modelling ice flow and radio-active decay of naturally abundant isotopes. Accelerator mass spectrometry enables to measure the $^{14}C/^{12}C$ ratio of graphite samples of as little as 30 micrograms, extracted from $CO_2$ in the air bubbles included in the ice cores. Ice samples have been dated at more than 24 kyr BP with this method (Van Roijen, 1996). Besides dating of ice samples the method also provides means to estimate long-term ablation and accumulation (of the last 15 - 100 years) with reasonable accuracy (10 to 30%). The major source of $^{14}C$ contamination in the ice originates from *in situ* production of $^{14}C$ caused by penetration of cosmic rays in the ice.

The two drill sites for the 1997-98 expedition were chosen after carefully studying the results of the 1992-93 expedition. The shallow cores drilled in 1992-93 revealed the spatial distribution of the age and the ablation rates in the Scharffenbergbotnen BIA. A logical continuation of this research is to try to reveal the age distribution with depth. To this end, two drill sites were selected where 100 m deep ice cores should be taken. One drill site was chosen near the equilibrium line separating the main BIA from the surrounding snow fields. In general the time range spanned by an ice core is largest at the equilibrium line, as can be deduced from ice dynamical modelling. This core will hopefully tell us more about the accuracy that can be achieved with the present $^{14}C$ method.

The second blue ice core was drilled close to the icefall (near drill site 6 in the 1992-93 season). The main aim of this core is to study in more detail the influx of ice from this side of the valley, as this influx may have varied over time. For instance, the ice mass flux from the icefall into the Scharffenbergbotnen valley may have been far greater during periods when the regional ice level was higher. It is hoped that signatures of such events can be traced back in this ice core.

Another important question that came up five years ago was the hypothesis of a constant production ratio of *in situ* produced $^{14}CO_2$ and $^{14}CO$. The basic principle of the method is that the total *in situ* produced $^{14}C$ can be determined by the measured amount of $^{14}CO$, since atmospheric $^{14}CO$ in ice is negligible and its presence is ascribed to *in situ* production. Van Roijen (1996) calculated an average value for the ratio between $^{14}CO_2$ and $^{14}CO$ of $3.8 \pm 0.8$. So far it can only be assumed that this value also holds for the accumulation area. By analysing samples of the transition zone (the zone where pore close-off occurs) of the EPICA cores (see section 6.3) we want to investigate if this assumption is justified.

## 6.2 Equipment

The drill used for the medium-deep coring is identical to the one successfully used by the BAS (British Antarctic Survey) in the Antarctic, which is developed with the aid of R. Mulvaney from BAS. The drill itself consists of an engine compartment, an anti-torque section, and a 2 meter barrel where the ice sample is collected. The drill head is mounted on an inner barrel that is taken out after each run to remove the ice core. A winch with 230 meters cable takes the drill up and down the borehole. A Honda 4 kW generator powers the winch and the drill. All these parts (except for the generator) were manufactured in close co-operation with BAS. Drillings took place inside an especially made tent (length 11 m, width 4 m, height 2.4 m) to enable good working conditions independent of the weather (Fig. 19).

*Figure 18. Location of the drilling sites SBB 01 and SBB 02 in the Scharffenbergbotnen valley. k1, k2 (both 3 meter) and k3 (7 meter) are the shallow cores drilled during this expedition. Also shown are the locations of the ice coring activities in 1992-93 in the form of two transects, and the meteorological sites 1 and 3.*

In the spring of 1997, two test drillings were performed in Sweden and Svalbard. These tests gave quite successful results: for instance, in Svalbard ice coring progressed to a depth of 121 m. Typically, it takes 4 to 6 days (of 9 working hours) for an experienced team of four persons to drill a 100 meter ice core. The drilling progress obviously slows down when the firn density increases; therefore it took considerably longer when drilling started on blue ice instead of snow. The average length of each sample, usually broken into two pieces, was as much as 90 cm. The longest single blue ice sample was 194 cm.

### 6.3 Medium long ice coring

The table below summarises the results of the entire 1997-98 medium deep ice coring program. The program was split into two parts: apart from the two cores drilled in Scharffenbergbotnen (SBB 01 and SBB 02) three cores were drilled in the framework of the EPICA pre site survey 1997-98 (at CM and CV). Information on these three cores is added here because parts of the EPICA cores will also be used for $^{14}C$-analysis. SBB 02 is the only site where no EPICA AWS was placed (see chapter 5). The temperature at 10 m depth is measured by the thermistor strings of the AWSs in the borehole (at SBB 02 the 10 m temperature was measured once with a separate thermistor, which may have given a too low temperature). The sites 1090 and Svea cross designate the locations of AWSs 4 and 6 (see section 5). GPS locations and elevations were measured with an accuracy of approximately 10 cm. More information on the logistics and a time table can be found in chapter 2.

| Site | Location | Elevation (m a.s.l.) | Ice core length (m) | Days needed to drill core (s) | Temperature (10 m) (°C) |
|---|---|---|---|---|---|

| | | | | | |
|---|---|---|---|---|---|
| 1090 | 72° 45' 09" S, 15° 29' 56" W | 34 | | | -19.4 |
| CM | 73° 06' 19" S, 13° 09' 53" W | 363 | 2 x 105 | 9 | -17.8 |
| Svea cross | 74° 28' 53" S, 11° 31' 01" W | 1160 | | | -23.0 |
| SBB 01 | 74° 34' 40" S, 11° 02' 58" W | 1173 | 52 | 5 | -18.8 |
| SBB 02 | 74° 34' 00" S, 11° 07' 52" W | 1216 | 85 | 6 | -22.8 |
| CV | 76° 00' 01" S, 08° 03' 02" W | 2399 | 136.5 | 8 | -38.7 |

The drilling team arrived in Scharffenbergbotnen on 23 December 1997. After establishing camp the drilling of the first core started on Christmas Eve. At a depth of 52 meters the drilling came to a stop due to a serious technical problem with the drill. It appeared that meltwater ingress had caused rust in the release section of the drill, making it impossible to rotate. The following days it turned out that we were not able to fix it without some special tools, which had to be brought in from Wasa. Since weather conditions were unfavourable (too warm, causing meltwater to leak into the borehole) to continue drilling in Scharffenbergbotnen, it was decided to start the EPICA traverse to the plateau Amundsenisen one week earlier than planned. The drilling of the second blue ice core was postponed until the last week of January when temperatures were expected to be lower.

Upon arrival of the traverse party on 2 January the drill was repaired and kept working well during the rest of the expedition. During the traverse, a 136.5 meter core was drilled at the southernmost point of the traverse (CV). On 22 January the traverse party returned from the plateau Amundsenisen and the second core was drilled in Scharffenbergbotnen. On 28 January the drill hit a stone in the ice at a depth of 85 meters, which ended the drilling at SBB 02. Fortunately, no damage to the drill was done, and on 29 January the drill team left for Wasa where drillings started again at Camp Maudheimvidda (CM) on 31 January. On 9 February two cores of 105 meters each were completed at this location.

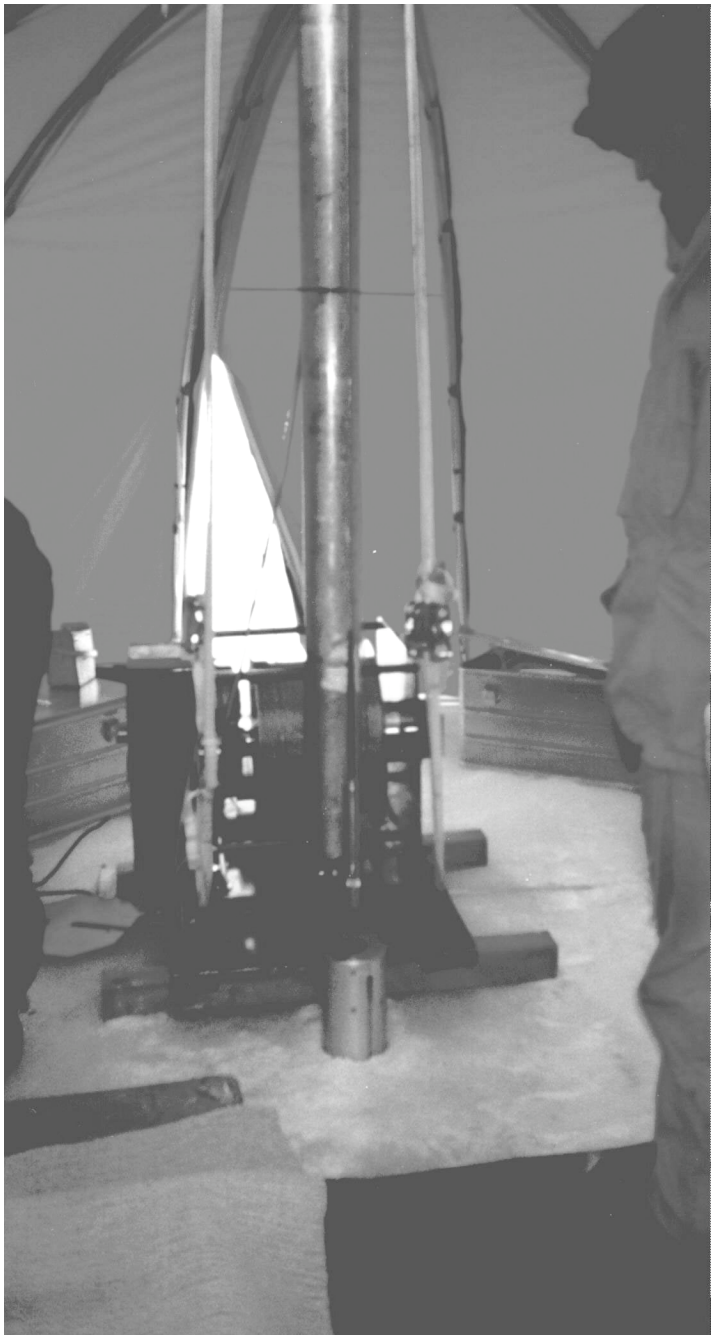

*Figure 19. Drilling inside the tent at the Scharffenbergbotnen BIA. The barrel in front of the winch is part of the drill sticking out of the bore hole.*

All cores, except those of SBB 01, were sealed in plastic and immediately stored in a small freezing container where the temperature was never higher than -16 °C. The cores from SBB 01 were first packed in boxes and dug into the snow at a depth of approximately 1.8 m. After the return from the plateau Amundsenisen these cores were also stored in the freezing container. All ice cores have been flown on board of the ship Outeniqua by helicopter and were stored in a freezing container at -20 °C. This container has been shipped to Stockholm (Sweden), from where

the ice samples will be distributed for analyses. The analyses of the blue ice cores will include $^{14}C$, DEP (di-electrical profiling), ECM (electrical conductivity measurement) and oxygen isotopes.

### 6.4 Shallow ice core drilling

Besides the two medium long cores also three additional shallow cores were drilled during this expedition (for their locations see Figure 18). In 1992-93 cores were drilled along two sections in Scharffenbergbotnen (see Figure 18). These sections probably both run approximately perpendicular to the isochrones (lines of equal age). A 7 m core was drilled in the area where the oldest ice (> 24 kyr) was found in 1992-93 (in a 3 m core), while two cores of 3 m length were drilled on the southern side of the coring transects of 1992-93. The 7 m core will be used to study the in situ produced $^{14}C$ in more detail. The same drill was used as five years ago. All locations were fixed with hand-held GPS-receivers.

## 7. Conclusions

The 97-98 field experiment can be considered successful, since virtually all research activities could be carried out as planned. In particular, the following issues were successfully achieved:

- Simultaneous atmospheric profile measurements at seven sites, four over snow and three over blue ice, during 37 days.
- Turbulence measurements over blue ice and snow during 40 days.
- Snowdrift profile measurements over blue ice and snow.
- Cable balloon soundings during eight complete days (eight soundings per day), one of which over blue ice and the rest near Svea.
- Radiosonde soundings during 39 days.
- Detailed surface albedo measurements (including broadband, narrow band and bi-directional reflection measurements) over blue ice and snow.
- Detailed blue ice ripple observations at five sites.
- Two medium-deep blue ice cores of 52 and 85 m depth.
- Three shallow blue ice cores.
- Three medium-deep firn cores of 105, 105 and 137 m length.

Undoubtedly, the meteorological measurements and ice-core drillings that were performed during the expedition will significantly enhance our knowledge on several issues concerning Antarctic blue ice areas. These include:

- atmospheric surface layer characteristics over blue ice and snow.
- surface energy balance of blue ice and snow.
- turbulence characteristics in the atmospheric surface layer over blue ice and snow.
- ablation and sublimation of blue ice, including their spatial distributions.
- snowdrift physics and transport rates over blue ice and snow.
- atmospheric boundary layer structure.

- mesoscale meteorological characteristics of western Dronning Maud Land.
- spectral and directional dependency of the albedo of snow and blue ice.
- the vertical and spatial distribution of the age of ice in a blue ice area.
- the vertical and spatial distribution of $CO_2$ and methane in the blue ice area.

## 8. Participants

*Meteorology:*
Richard Bintanja (field leader, post-doc)
Carleen Reijmer (PhD. student)
Henk Snellen (technician)

*Ice-core drilling:*
Martijn Thomassen (PhD. student), in co-operation with Lars Karlöf, Mart Nyman, Malin Stenberg and Knut Gjerde.

## Acknowledgements

We thank our Swedish, Norwegian and Finnish expedition colleagues of SWEDARP 1997-98 for their assistance, interest in our work and their pleasant company in general. In particular Lars Karlöf and Mart Nyman are thanked for their invaluable help with the ice core drilling, the erection of the EPICA weather stations and their assistance to find a safe route to sites 4 and 5. Furthermore, we are grateful to the South-African crew of the Outeniqua for their assistance in the logistic activities on the ship. Helmut Tüg and Heiko Lilienthal are thanked for supplying us with the snowdrift equipment. We thank the Royal Netherlands Meteorological Institute for giving access to their boundary layer research facility in Cabauw, the Netherlands. We are further grateful to the following persons and institutions:

J. Oerlemans, R. van de Wal, J. de Wolde, L. Conrads, S. Tijm, P. Duynkerke, IMAU, Utrecht University
W. Boot, M. Portanger, I. van Kooten, K. Haryachi, Electronical and Technical Assistance, IMAU, Utrecht University
G. Hörchner, W. Tijben, T. Vos, Technical Assistance, IGF, Utrecht University
P. Braams, Braams Techniek
A. van Londen and co-workers at the Calibration Division of the Royal Netherlands Meteorological Institute (De Bilt)
W. Kohsiek, Royal Netherlands Meteorological Institute (De Bilt)
R. Schorno (GOA), B. Sinke (NIO, Yerseke)
J. Meissner (Hafen Spedition, Bremerhaven)
V. Lander (Hagemann and Meihuizen, Cape Town)
P. Holmlund (Stockholm University, Stockholm)
R. Mulvaney (British Antarctic Survey, Cambridge)
H. Oerter (Alfred-Wegener-Institut, Bremerhaven)

We thank the members of the Swedish Polarforsknungssekretariat who were involved in the 1997-98 SWEDARP expedition, in particular Anders Modig, Tomas Karlberg, Claes Andersson, Ann-Sofie Rickby and Olle Melander.

We thank the following companies for there co-operation:
Mierij Meteo, Kettlitz & Deenik Insurance-broker, Donex Shipping and Forwarding, Institut für Angewandte Geodäsie, Air Products.

Financial support was provided by the Netherlands Antarctic Programme of the Netherlands Organisation for Scientific Research (NWO) and the European Project for Ice Coring in Antarctica (EPICA) under EU contract ENV4-CT95-0074.

## References

Bintanja, R., M.R. van den Broeke and M.J. Portanger, 1993: A meteorological and glaciological experiment on a blue ice area in the Heimefront Range, Queen Maud Land, Antarctica. *Svea Field Report*, Institute for Marine and Atmospheric Research Utrecht, Utrecht University, 29 pp.

Bintanja, R., M.R. van den Broeke and M.J. Portanger, 1995: Meteorological and glaciological investigations in Scharffenbergbotnen, Heimefrontfjella, Dronning Maud Land. In: *Swedish Antarctic Research Programme 1992/93: A Cruise Report*. M. Lönnroth Carlson (Ed.), Swedish Polar Research Secretariat, Stockholm, 21-44.

Bintanja, R. and M.R. van den Broeke, 1994: Local climate, circulation and surface energy balance of an Antarctic blue ice area. *Ann. Glaciol.*, **20**, 160-168.

Bintanja, R. and M.R. van den Broeke, 1995a: The surface energy balance of Antarctic snow and blue ice. *J. Appl. Meteorol.*, **34**, 902-926.

Bintanja, R. and M.R. van den Broeke, 1995b: Momentum and scalar transfer coefficients over aerodynamically smooth Antarctic surfaces. *Boundary-Layer Meteorol.*, **74**, 89-111.

Bintanja, R. and M.R. van den Broeke, 1995c: The climate sensitivity of Antarctic blue ice areas. *Ann. Glaciol.*, **21**, 157-161.

Bintanja, R., S. Jonsson and W.H. Knap, 1997: The annual cycle of the surface energy balance of Antarctic blue ice. *J. Geophys. Res.*, **102**, 1867-1881.

Bintanja, R., 1998: On the glaciological, meteorological and climatological significance of Antarctic blue ice areas. *J. Geophys. Res.* (submitted).

Greuell, W., M. van den Broeke, W. Knap, C. Reijmer, P. Smeets and I. Struijk, 1995: PASTEX: A glacio-meteorological experiment on the Pasterze (Austria). Institute for Marine and Atmospheric Research Utrecht, Utrecht University, 34 pp.

Jonsson, S. 1992. Local climate and mass balance of a blue-ice area in Western Dronning Maud Land, Antarctica. *Zeitschrift für Gletscherkunde und Glazialgeologie,* **27**, 11-29.

Jonsson, S. 1995. Synoptic forcing of wind and temperature in a large cirque 300 km from the coast of East Antarctica. *Antarctic Science*, **7**, 409-420.

Kaimal, J.C. and J.J. Finnigan, 1994: *Atmospheric boundary layer flows: their structure and measurement*. Oxford University Press, USA, 289 pp.

Knap, W.H., C.H. Reijmer, J. Oerlemans, 1997: Narrow band to broad band conversion of Landsat-TM glacier albedos. *International Journal of Remote Sensing*. (submitted).

Knap, W.H., C.H. Reijmer, 1997: Anisotropy of the reflected radiation field over melting glacier ice: measurements in Landsat-TM bands 2 and 4. *Remote Sensing of Environment*. (accepted).

Knap, W.H., 1997: Satellite-derived and ground-based measurements of the surface albedo of glaciers. Ph.D Thesis, Utrecht University, 175 pp.

Oerlemans, J., H. Björnson, M. Kuhn, F. Obleitner, F. Palsson, P. Smeets, H.F. Vugts and J. de Wolde, 1998: A glacio-meteorological experiment on Vatnajökull, Iceland. *Boundary-Layer Meteorol.*, (submitted).

Pomeroy, J. W., and D. M. Gray, 1990: Saltation of snow. *Water Resources Res.*, **26**(7), 1583-1594.

Pomeroy, J. W., and D. H. Male, 1992: Steady-state suspension of snow. *J. Hydrol.*, **136**(1-4), 275-301.

Struijk, I., 1996: Test phase of the Campbell sonic anemometer in Cabauw. Institute for Marine and Atmospheric Research Utrecht, Report V 96-19, 44 pp.

Van den Avoird, E., 1997:Turbulence in a katabatic flow: measurements on the Vatnajökull Ice Cap, Iceland. Institute for Marine and Atmospheric Research Utrecht, Report V 97-5, 49 pp.

Van den Broeke, M.R. and R. Bintanja, 1995a: Summertime atmospheric circulation in the vicinity of a blue ice area in East Queen Maud Land, Antarctica. *Boundary-Layer Meteorol.*, **72**, 411-438.

Van den Broeke, M.R. and R. Bintanja, 1995b: On the interaction of katabatic wind and blue ice area formation in East-Antarctica. *J. Glaciol.*, **41**, 395-407.

Van den Broeke M.R., J.-G Winther, E. Isaksson, F. Pinglot, T. Eiken and L. Karlöf, 1998: Climate variables along a traverse line in Dronning Maud Land, East Antarctica. *submitted to J. of Glaciology.*

Van Roijen, J.J., 1996: *Determination of Ages and Specific Mass Balances from $^{14}C$ Measurements on Antarctic Surface Ice*. Ph.D. Thesis, Utrecht University, 119 pp.

Van Roijen, J. J., K. van den Borg, A. F. M. de Jong and J. Oerlemans, 1995: Ages and ablation and accumulation rates from $^{14}C$ measurements on Antarctic ice. *Ann. Glaciol.*, **21**, 139-143.

Tüg, H., 1988: A pulse-counting technique for the measurement of drifting snow. *Ann. Glaciol.*, **11**, 184-186.